

**Aus der Klinik für Pferde, Allgemeine Chirurgie und Radiologie
des Fachbereichs Veterinärmedizin
der Freien Universität Berlin**

New Surgical Techniques of Equine Cervical Spine Surgery in Horses

**Inaugural-Dissertation
zur Erlangung des Grades eines
Doctor of Philosophy (PhD)
in Biomedical Sciences
an der Freien Universität Berlin**

**vorgelegt von
Dr. med. vet. Nicole Schulze, geb. Guhl
Tierärztin aus Hagenow**

**Berlin 2022
Journal-Nr.: 4367**

Aus der Klinik für Pferde, Allgemeine Chirurgie und Radiologie
des Fachbereichs Veterinärmedizin
der Freien Universität Berlin

New Surgical Techniques of Equine Cervical Spine Surgery in Horses

Inaugural-Dissertation

zur Erlangung des Grades eines
Doctor of Philosophy (PhD)
in Biomedical Sciences
an der Freien Universität Berlin

vorgelegt von

Dr. med. vet. Nicole Schulze, geb. Guhl

Tierärztin aus Hagenow

Berlin 2022

Journal-Nr. 4367

Gedruckt mit Genehmigung
des Fachbereichs Veterinärmedizin
der Freien Universität Berlin

Dekan: Univ.-Prof. Dr. Uwe Rösler
Erster Gutachter: Univ.-Prof. Dr. Christoph Lischer
Zweiter Gutachter: Prof. Dr. Leo Brunnberg
Dritter Gutachter: Univ.-Prof. Dr. Mahtab Bahramsoltani

Deskriptoren (nach CAB- Thesaurus): horses, osteoarthritis, osteochondritis
dissecans (MeSH), spine, spinal diseases, surgery, veterinary practice, arthroscopy
(MeSH), computed tomography

Tag der Promotion 12. Oktober 2022

Gewidmet Klaus Guhl

Zeit heilt keine Wunden, sie macht es nur erträglicher.

Inhaltsverzeichnis

List of abbreviations	II
1 Introduction	1
2 Literature	3
2.1 Anatomy and Biomechanics of the Equine Cervical Spine.....	3
2.2 Computed Tomographic Examination of the Equine Cervical Spine	5
2.3 Pathology of the Equine Cervical Spine	6
2.3.1 Cervical vertebral stenotic myelopathy	6
2.3.2 Fracture and Luxation of the cervical vertebrae.....	6
2.3.3 Pathologies of the APJs.....	7
2.4 Surgical Treatment Options of Pathologies of the Equine Cervical Spine.....	8
3 Research publications in peer-reviewed journals	11
3.1 Computed Tomographic Evaluation of Adjacent Segment Motion after Ex Vivo Fusion of Equine Third and Fourth Cervical Vertebrae	11
3.2 Dynamic three-dimensional computed tomographic imaging facilitates evaluation of the equine cervical articular process joint in motion.....	21
3.3 Internal fixation of a complete ventral luxation of the dens axis in an American quarter horse yearling	31
3.4 Arthroscopic removal of osteochondral fragments of the cervical articular process joints in three horses.....	39
4 Discussion	49
5 Zusammenfassung	55
6 Summary	57
7 Literaturverzeichnis	59
8 List of publications and oral presentations	71
9 Danksagung	73
10 Funding Sources	74
11 Conflict of Interest	75
12 Selbstständigkeitserklärung	76

List of abbreviations

APJ	Articular process joint
ASD	Adjacent segment disease
CT	Computed tomography
CVM	Cervical vertebral malformation
CVSM	Cervical vertebral stenotic myelopathy
LCP	Locking compression plate
MS	Motion segment
OA	Osteoarthritis
OCD	Osteochondrosis dissecans
T-LCP	T- Locking compression plate
3D	Three-dimensional
2D	Two-dimensional

1 Introduction

The cervical spine is receiving increased attention as a source of dysfunction in the equine patient. In the last years the availability of large, computed tomography (CT) gantry apertures in several equine referral centers makes detailed multidimensional diagnostic imaging of the equine cervical spine more applicable. This allows more accurate and improved detection of cervical spine lesions. While there are some studies detailing the CT anatomy as well as pathological findings in the equine cervical spine, little is known about the exact interaction, movement pattern and range of motion of the cervical articular process joints.

Common pathological conditions include cervical vertebral fractures, luxations as well as developmental cervical vertebral malformations. Osteochondrosis dissecans (OCD), OCD-like lesions and osteoarthritis (OA) of the cervical articular process joint (APJ) also play a significant role (Stewart et al. 1991). These disorders can limit athletic activity and lead to clinical signs like weakness, proprioceptive deficits, ataxia, decreased cervical range of motion, decreased performance and forelimb lameness (Powers et al. 1988; Jane et al. 2015; Trostle et al. 1993; Ricardi et al. 1993).

Depending on the cause of the pathology, surgical techniques include ventral cervical fusion of the equine cervical vertebrae or arthroscopy of the cervical APJs (Pepe et al. 2014; Grant et al. 1985; Walmsley et al. 2005; Moore et al. 1993). Fusion of the cervical spine in horses was first published in 1985 for cases with cervical vertebral stenotic myelopathy (CVSM) and has been described using various techniques (Grant et al. 1985; Walmsley et al. 2005; Moore et al. 1993). Fusion of the human cervical spine may result in adjacent segment disease (ASD) characterized by pathologic processes such as joint and disc degeneration in the motion segments (MS) adjacent to the fused MS (Ahmed et al. 2017).

To our knowledge, there are no studies in equine medicine about the investigation of the possible development of this pathology after cervical spine fusion in horses.

Some time ago, arthroscopy of the APJs of the neck has been investigated. The arthroscopic anatomy of APJs has been described in cadavers and in 3 clinical cases (Pepe et al. 2014). Additionally, a “cut down” arthroscopic approach for OCD fragment removal has been described in one horse (Tucker et al. 2018). In three out of the four clinical cases, the horses were euthanized shortly after surgery due to deteriorating clinical signs or a poor prognosis for athletic activity. In a recently published study, multiple osteochondral fragments were successfully removed from the caudal APJs in 6 horses with a combination of “cut down”

approach and arthroscopy. All horses returned to ridden work postoperatively (Tucker et al. 2021).

The first aim of this study was to investigate the feasibility of dynamic CT for diagnostic imaging of the equine cervical APJs and to give a detailed description of APJ movement in a cadaver model. We hypothesized that dynamic CT facilitates the comprehensive assessment of the equine cervical APJ components in motion. The second aim of this study was to evaluate the momentary state of the biomechanical impact of cervical vertebral fusion on adjacent motion segments in the horse. The authors hypothesized that the range of motion of the C2/3 and C4/5 segments will increase when force is applied in flexion and extension, as well as in lateral bending after cervical fusion of C3/4 using locking compression plate fixation.

In addition, we were able to report the first case series describing successful arthroscopic removal of osteochondral fragments in the APJs of the equine cervical spine, and report of a successful surgical treatment of a complete luxation of the atlantoaxial articulation with a 4.5-mm T-locking compression plate (T-LCP) in a horse.

2 Literature

2.1 Anatomy and Biomechanics of the Equine Cervical Spine

The equine cervical spine is formed of 7 cervical vertebrae. The basic bone structure of the vertebrae consists of the vertebral body, the vertebral arch and the various vertebral processes (Wissdorf et al. 2010). The dorsally located vertebral arch, formed by bilateral bony laminae, surrounds and protects the spinal cord and adjacent structures. The vertebral bodies from C3-C7 have a convex cranial surface, the head, and a corresponding concave caudal surface, the fossa. The connection between the cranial surface (head) and the caudal surface (fossa) of the two vertebral bodies is mediated by an intervertebral disc (Wissdorf et al. 2010). The length of the body of the equine cervical spine decreases caudally.

The third to seventh cervical vertebrae each have pairs of cranial and caudal articular processes projecting from the borders of the vertebral arch while the second cervical vertebra has a caudal articular process only (Wissdorf et al. 2010; Hensen et al. 2018; Butler et al. 2016). The extremities of these processes carry articular surfaces, which articulate with those of adjacent vertebrae, forming the equine cervical APJs. These joints are bilateral intervertebral synovial diarthroses lined with hyaline cartilage (Henson et al. 2018; O'Leary et al. 2018; Nickel et al. 1986). The APJs are located dorsal to the intervertebral foramen and extend medially towards the vertebral canal (Claridge et al. 2010). Caudal to the atlantoaxial articulation the joint surfaces are oriented obliquely, at approximately 45°–55° to the horizontal plane, which increases further caudally as it progresses (Whithers et al. 2009).

The first two vertebrae, termed atlas and axis, have a unique morphology compared with the rest of the equine cervical spine (Wissdorf et al. 2010; Hensen et al. 2018).

The first cervical vertebra has no body or articular processes. The second cervical vertebra is characterized by the *dens axis*, which rests in a concavity at the ventral aspect of the atlas and is held in place by several ligaments. The dens fuses with the head at approximately 7 months of age (Wissdorf et al. 2010; Hensen et al. 2018; Butler et al. 2016). The sixth cervical vertebra has a pronounced paired ventral lamina. (Wissdorf et al. 2010; Hensen et al. 2018). The seventh cervical vertebra is shorter than the sixth and may have a small spinous process dorsally which varies in size, shape and position among horses (Wissdorf et al. 2010; Hensen et al. 2018).

The spinal cord discharges eight paired cervical nerves, each consisting of a ventral and a dorsal branch (Wissdorf et al. 2010).

The first and second cervical nerves exit the spinal canal through the lateral vertebral holes of the axis and atlas, respectively. Between C3 and C7, the respective cervical nerves exit into the periphery through the associated intervertebral foramen (Wissdord et al. 2010). The eighth cervical nerve runs caudal to the last cervical vertebra (De Lahunta et al. 2014b).

Two adjacent articulating vertebrae and the connecting tissues binding them build a functional unit called spinal motion segment (MS). The difference between full extension and flexion and right and left lateral bending is defined as range of motion of the spinal MS (Yoon et al. 2006). There are three main types of movement in the motion segments of the equine cervical spine: flexion and extension, lateral flexion, and axial rotation. Vertical and transverse translation as well as longitudinal compression have also been described but play a minor role in the range of motion of the equine cervical spine (Krüger et al. 1939; Clayton et al. 1989a; Zsolodos et al. 2015).

The range of motion of the seven cervical vertebrae in these 3 movement types has major effects on the horse's locomotor system, as the neck acts as a lever and supports the horse's balance (Krüger et al. 1939; Clayton et al. 1989a; Zsolodos et al. 2015).

As described earlier, the first two vertebrae of the cervical spine have a unique morphology that also differs from the other vertebrae in the specific types of movement (Wissdord et al. 2010; Hensen et al. 2018). Compared to the other cervical spine MSs, the atlantooccipital joint has the largest dorsoventral flexion-extension range of motion. The maximum rotational movement occurs between C1 and C2 (Clayton et al. 1989a). An increase in range of motion from the cranial to the caudal MSs (C2/3–C6/7) for dorsoventral flexion-extension as well as lateral bending was found in cadaveric studies (Clayton et al. 1989a). However, in an *in vivo* study more range of motion was observed in the cranial cervical spine for dorsoventral flexion-extension (C1/2–C4/5), while C5/6 showed the smallest range of motion in dorsoventral flexion-extension, rotation and lateral bending both directions (Zsolodos et al. 2015).

2.2 Computed Tomographic Examination of the Equine Cervical Spine

Diagnosis of cervical spine disease in the horse is a clinical challenge. The sensitivity and specificity of routine imaging techniques such as radiography, ultrasound, and nuclear scintigraphy are severely limited due to complex anatomy and superimpositions (Dimock and Puchalski 2010). The recent adaptation of CT scanners and the availability of large CT gantry aperture makes detailed multidimensional diagnostic imaging of the entire equine cervical spine possible (Tucker et al. 2020; Lindgren et al. 2020; Gough et al. 2020).

Another innovation in computed tomography is the dynamic three-dimensional (3D) reconstruction of CT images, which is not yet used in veterinary medicine. In human orthopedics, this technique is increasingly used and enjoys great popularity (Gondim et al. 2017; Kerkhof et al. 2016). Dynamic CT allows, evaluation of anatomical structures in motion as multiple image volumes are recorded over time and subsequently reviewed in form of a video sequence (White et al. 2019). The acquired dataset can be examined either as a dynamic 3D volume-rendered view (dynamic 3D CT) or a dynamic 2D cross-section in any imaging plane (dynamic 2D CT) (Alta et al. 2012).

Dynamic 3D CT is of particular interest in human medicine for conditions with a dynamic component, such as bone impingement, intra-articular ligamentous insufficiency, dynamic instability syndromes, and dynamic vascular compression in (Chois et al. 2013; Gondim et al. 2017; Leng et al. 2011).

Several studies have already demonstrated the potential of dynamic 3D CT for the assessment of the human wrist, shoulder, knee, and hip in motion (Leng et al. 2011; Edirisinghe et al. 2014; Tay et al. 2007; Totterman et al. 1998; Wassilew et al. 2013). Thus, this imaging technique also appears promising in veterinary medicine.

2.3 Pathology of the Equine Cervical Spine

2.3.1 Cervical vertebral stenotic myelopathy

Often, pathologies of the equine cervical spine result in compression of the spinal cord, which in the worst case can lead to pronounced clinical neurological symptoms. Peripheral nerve compression without spinal cord compression may also cause similar clinical symptoms (Nixon et al. 1982; Ricardi and Dyson 1993; Rush 2003). A recent study has already demonstrated by CT that APJ pouches can extend into the vertebral canal, highlighting the potential of an APJ effusion to cause spinal cord compression (Claridge et al. 2010). These disorders can limit athletic activity and lead to clinical signs like weakness, proprioceptive deficits, ataxia, decreased cervical range of motion, decreased performance and forelimb lameness (Powers et al. 1988; Jane et al. 2015; Trostle et al. 1993; Ricardi et al. 1993).

Both, compression of the spinal cord and peripheral nerves can be caused by fractures, luxation / subluxation, developmental abnormalities like cervical vertebral stenotic myelopathy (CVSM) and degenerative changes of the APJs, among others (Funk and Erickson 1968; Auer and Stick 2018; Powers et al. 1986; García-López 2018; Dyson 2011; Stewart 1991; Ricardi and Dyson 1993; Trostle et al. 1993).

Two types of CVSM syndromes are distinguished. The first is a static stenosis. Here, compression occurs regardless of the position of the neck in the region of the caudal cervical vertebrae C5-C7. In contrast, the second type is dynamic compression, which is usually increased during flexion and is predominantly found in the mid-cervical area (Moore et al. 1993).

2.3.2 Fracture and Luxation of the cervical vertebrae

Fractures and luxation of the cervical vertebral differ considerably from those of other skeletal bones. On the one hand, they occur less frequently and on the other hand, they are more difficult to diagnose. In general, younger horses are more frequently affected (Mayhew 1978; Auer and Stick 2018). Fractures of the dens with atlantoaxial subluxation are most seen in foals younger than 6 months of age, although they can also occur in adult horses (Slone et al. 1973; McCoy et al. 1984; Levine et al. 2007; Auer and Stick 2018). Nevertheless, subluxation or luxation of the atlantoaxial articulation are an uncommon pathology in the horse (Slone et al. 1973; McCoy et al. 1984; Levine et al. 2007; Auer and Stick 2018). They can be caused by congenital defects or be a result from a traumatic

incident (Slone et al. 1973; McCoy et al. 1984; Funk and Erickson 1968; Auer and Stick 2018; Witte et al. 2005; Ehrle et al. 2012; Nixon 1996; Nixon and Stashak 1988).

The dens axis is connected to the atlas and the occiput of the skull. If all the ligaments (apical, transverse, and alar ligaments) rupture, it is called a complete luxation of the atlantoaxial articulation (Nickel 1986; McCoy et al. 1984; Witte et al. 2005; Slone et al. 1973). As a consequence, the dens lies ventral to the atlantic arch, which leads to instability of the articulation and can cause spinal cord compression (Funk and Erickson 1968).

2.3.3 Pathologies of the APJs

Pathological conditions of the APJs include OCD, OCD-like lesions, fracture, and OA (Pool 1993; Rooney 1975; Powers et al. 1988; Tucker et al. 2018; Beck et al. 2002; Bergmann et al. 2020; Limet al. 2017; Janes et al. 2015). Because of the proximity to the spinal cord these disorders can limit athletic activity and lead to clinical signs like decreased cervical range of motion, forelimb lameness, weakness, proprioceptive deficits, and ataxia (Powers et al. 1988; Jane et al. 2015; Trostle et al. 1993; Ricardi et al. 1993).

Pathologies of the APJs implicated in the etiology of cervical vertebral malformation (CVM) include OC and OA of the APJs (Powers et al. 1986; Stewart et al. 1991; Moore et al. 1992, 1994; Trostle et al. 1993; Mattoon et al. 2004). Fractures, OC, OA and CVM have been reported to be associated with joint effusion, new bone formation, joint capsule hypertrophy, ligament flavum hypertrophy, dorsal lamina hypertrophy and synovial cysts (Powers et al. 1986; Trostle et al. 1993; McIlwraith and Trotter 1996; McIlwraith et al. 2001). The etiology behind osteochondral fragments of cervical APJs is not yet fully understood. OCD and OCD-like lesions, as well as osteochondromatosis and fragmentation secondary to trauma are suggested as possible sources for these fragments (Tucker et al. 2018; Lim et al. 2017; Tucker et al. 2021; Moore et al. 1992).

2.4 Surgical Treatment Options of Pathologies of the Equine Cervical Spine

Successful treatment of pathologies compressing the spinal cord and peripheral nerves remains a challenge. Moreover, the success is critically questioned (Nout and Reed 2003; Van Biervliet et al. 2006; Levine et al. 2008). Currently, conservative therapy, euthanasia, or surgical management have been described (Mayhew et al. 1993; Trostle et al. 2003). Depending on the cause of the pathology, surgical options include ventral cervical fusion of the equine cervical vertebrae and arthroscopy of the cervical APJs (Pepe et al. 2014; Grant et al. 1985; Walmsley et al. 2005; Moore et al. 1993).

For the fusion of two or more cervical vertebrae surgical techniques described include the use of locking compression plates, stainless steel Cloward Bagby baskets, titanium-based kerf cut cylinders or a polyaxial pedicle screw and rod construct (Walmsley et al. 2005; Moore et al. 1993; Reardon et al. 2009; Reardon et al. 2010; Aldrich et al. 2018; Kühnle et al. 2018). The implantation of a titanium-based, threaded kerf-cut cylinder is the most popular and refined option available (Szklarz et al. 2017, Auer and Stick 2018).

Locking compression plate fusion had similar mechanical properties to the use of a kerf cut cylinder in a biomechanical evaluation in cadaveric specimens which may justify its use in clinical cases (Reardon et al. 2010).

Ventral cervical fusion is also the treatment of choice for subluxations such as an atlantoaxial subluxations or luxation / subluxation of the more caudally located cervical vertebrae (Funk and Erickson 1968; Auer and Stick 2018). However, no surgical treatment has yet been described for complete luxation of the articulation between the atlas and axis (Fürst 2019).

Fusion of the human cervical spine may result in ASD characterized by pathologic processes such as joint and disc degeneration in the MS adjacent to the fused MS. The condition is thought to be caused by an increase in range of motion and higher loads acting upon adjacent motion segments after intervertebral fusion (Ahmed et al. 2017). A higher incidence of adjacent segment disease has been observed when plates were used instead of kerf cut cylinder for intervertebral fusion in humans (Ahmed et al. 2017). The compensatory increase in motion of C4/5 was also observed in a canine cadaveric study after fusion of C5/6 (Hokazaki et al. 2017). As cervical fusion is performed in horses with various pathological conditions, it is plausible that adjacent segment disease is of concern in horses as well.

The success rate for cervical ventral fusion, regardless of the method chosen, has been reported in the literature to be 43-79% (Moore et al. 1993; Schütte 2005; Walsmley et al.

2005; Grant et al. 1985; Nixon and Stashak 1985; Grant et al. 2003). One of the main reasons for complications is implant failure and vertebral body fractures of the adjacent vertebrae (Szkwarz et al. 2018; Moore et al. 1993; Walmsley 2005; Grant et al. 1985; Grant et al. 2003; Nixon et al. 1985).

While ventral cervical fusion has been performed in equine surgery for some time, the arthroscopic approach and anatomy of cervical APJ has only recently been described (Pepe et al. 2014). In clinical cases diagnostic arthroscopy of articular process joints has been described in three horses as well as a “cut down” arthroscopic approach for OCD fragment removal in one horse (Tucker et al. 2018; Pepe et al. 2014). In three out of the four reported cases, the horses were euthanized shortly after surgery due to deteriorating clinical signs or a poor prognosis for athletic activity.

The treatment of choice for the majority of osteochondral fragments located in other equine joints is arthroscopic removal (McIlwraith 2013; McIlwraith et al. 1991).

3 Research publications in peer-reviewed journals

3.1 Computed Tomographic Evaluation of Adjacent Segment Motion after Ex Vivo Fusion of Equine Third and Fourth Cervical Vertebrae

Authors: Nicole Schulze; Anna Ehrle; Renate Weller; Guido Fritsch; Jennifer Gernhardt; Racem Ben Romdhane; Christoph J. Lischer

Publication: Veterinary and Comparative Orthopaedics and Traumatology. 2020; 33: 1-8.

DOI: 10.1055/s-0039-1693665

Correspondence Address:

Dr. med. vet. Nicole Schulze

Klinik für Pferde

Fachbereich Veterinärmedizin

Freie Universität Berlin, Oertzenweg 19B, 14163 Berlin

Phone: +49 30 838 622 99

Fax: +49 30 838 625 29

Email: nicole.schulze@fu-berlin.de

Authorship: All authors contributed to the study design and interpretation of the data. N. Schulze, A. Ehrle and C. Lischer were mainly responsible for the planning of the project as well as data acquisition, analysis and interpretation. G. Fritsch and J. Gernhardt contributed to the study execution and data analysis. R. Weller developed the described image analysis and R. Ben Romdhane was mainly responsible for data acquisition and statistical analysis. All authors approved the final version of the manuscript.

You have to purchase this part online.

3.2 Dynamic three-dimensional computed tomographic imaging facilitates evaluation of the equine cervical articular process joint in motion

Authors: Nicole Schulze; Natasha Werpy; Jennifer Gernhardt; Guido Fritsch; Thomas Hildebrandt; Katrien Vanderperren; Robert Klopfleisch; Racem Ben Romdhane; Christoph J. Lischer; Anna Ehrle

Publication: Equine Veterinary Journal 2022; DOI: 10.1111/evj.13560

Correspondence Address:

Dr. med. vet. Nicole Schulze

Klinik für Pferde

Fachbereich Veterinärmedizin

Freie Universität Berlin, Oertzenweg 19B, 14163 Berlin

Phone: +49 30 838 622 99

Fax: +49 30 838 625 29

Email: nicole.schulze@fu-berlin.de





Authorship: All authors contributed to the study design and interpretation of the data.

N. Schulze, A. Ehrle and N. Werpy were mainly responsible for the planning of the project as well as data acquisition, analysis and interpretation. G. Fritsch, R. Klopfleisch, J. Gernhardt, C. Lischer and T. Hildebrandt contributed to the study execution and data analysis. K.

Vanderperren and N. Werpy developed the described image analysis and R. Ben Romdhane was mainly responsible for data acquisition and statistical analysis. All authors approved the final version of the manuscript.

ORIGINAL ARTICLE

Dynamic three-dimensional computed tomographic imaging facilitates evaluation of the equine cervical articular process joint in motion

Nicole Schulze¹  | Natasha Werpy² | Jennifer Gernhardt¹ | Guido Fritsch³ | Thomas Hildebrandt³ | Katrien Vanderperren⁴ | Robert Klopfleisch⁵  | Racem Ben Romdhane⁶  | Christophorus Lischer¹ | Anna Ehrle¹ 

¹Equine Clinic, Surgery and Radiology, Freie Universität Berlin, Berlin, Germany

²Equine Diagnostic Imaging Inc., Archer, Florida, USA

³Leibniz Institute for Zoo and Wildlife Research, Forschungsverbund Berlin e.V., Berlin, Germany

⁴Department of Veterinary Medical Imaging and Small Animal Orthopaedics, Ghent University, Ghent, Belgium

⁵Institute for Veterinary Pathology, Freie Universität Berlin, Berlin, Germany

⁶Institute for Veterinary Epidemiology and Biostatistics, Freie Universität Berlin, Berlin, Germany

Correspondence

Nicole Schulze, Equine Clinic, Surgery and Radiology, Freie Universität Berlin, Berlin, Germany.

Email: nicole.schulze@fu-berlin.de

Funding information

European College of Veterinary Surgeons (ECVS Residents Research Grant).

Summary

Background: Dynamic computed tomography (CT) imaging has been introduced in human orthopaedics and is continuing to gain popularity. With dynamic CT, video sequences of anatomical structures can be evaluated in motion.

Objectives: To investigate the feasibility of dynamic CT for diagnostic imaging of the equine cervical articular process joints (APJs) and to give a detailed description of the APJ movement pattern.

Study design: Descriptive cadaver imaging.

Methods: Cervical specimens of twelve Warmblood horses were included. A custom-made motorised testing device was used to position and manipulate the neck specimens and perform dynamic 2D and 3D CT imaging. Images were obtained with a 320-detector-row CT scanner with a 160 mm wide-area (2D) solid-state detector design that allows image acquisition of a volumetric axial length of 160 mm without moving the CT couch. Dynamic videos were acquired and divided into four phases of movement. Three blinded observers used a subjective scale of 1 (excellent) to 4 (poor) to grade the overall image quality in each phases of motion cycle.

Results: With an overall median score of 1 the image quality, a significantly lower score was observed in the dynamic 3D videos over the four phases by the three observers compared with the 2D videos for both flexion (3D 95% CI: 1-2 and 2D 95% CI: 1-3; $P = .007$) and extension movement (3D 95% CI: 1-2 and 2D 95% CI: 1-3; $P = .008$). Median Translational displacement of the APJ surface was significantly greater in flexion than in extension movement ($P = .002$).

Main limitations: The small number of specimens included. Excision of spines and removal of musculature.

Conclusions: The study is a first step in the investigation of the potential of dynamic 3D CT in veterinary medicine, a technique that has only begun to be explored and leaves much room for refinement prior to its introduction in routine practice. CT with

This is an open access article under the terms of the Creative Commons Attribution License, which permits use, distribution and reproduction in any medium, provided the original work is properly cited.

© 2022 The Authors. *Equine Veterinary Journal* published by John Wiley & Sons Ltd on behalf of EVJ Ltd.

a detector coverage of 16 cm and a rotation speed of 0.32 seconds provides high-quality images of moving objects and gives new insight into the movement pattern of equine cervical APJs.

KEYWORDS

articular process joints, cervical spine, dynamic computed tomography, horse, image quality

1 | INTRODUCTION

Three-dimensional (3D) reconstruction of computed tomographic (CT) images can be used in presurgical planning and has other applications in veterinary patients.¹ Dynamic CT imaging has been introduced in human orthopaedics over the past decade and is continuing to gain popularity, but the technique is not yet utilised in veterinary medicine.^{2,3} With dynamic CT, anatomical structures can be evaluated in motion as multiple image volumes are recorded over time and subsequently reviewed in form of a video sequence.⁴ The acquired dataset can be examined either as a dynamic 3D volume-rendered view (dynamic 3D CT) or a dynamic 2D cross-section in any imaging plane (dynamic 2D CT).⁵

The application of dynamic 3D CT is of interest, especially for the investigation of musculoskeletal diseases with a dynamic component like bone impingement, intra-articular ligament sufficiency, dynamic instability syndromes and dynamic vascular compression in man.⁶⁻⁸ Several studies have demonstrated the potential of dynamic 3D CT for the evaluation of the human wrist, shoulder, knee and hip in motion.⁸⁻¹³

The cervical spine and particularly the articular process joints (APJs) are currently receiving increased attention as a source of dysfunction in the equine patient.¹⁴⁻¹⁹ The range of motion (ROM) of the cervical spine has major implications for the coordination and balance of the equine locomotor system and the availability of large CT gantry apertures in several equine referral centres makes detailed multidimensional diagnostic imaging of the equine cervical spine more applicable.¹⁹⁻²² Whilst there are some studies detailing the CT anatomy as well as pathological findings in the equine cervical spine, little is known about the exact interaction, movement pattern and ROM of the cervical APJs during dorsoventral flexion-extension and lateral bending.²³⁻²⁵

Pathological conditions of the equine cervical APJs include osteochondrosis, fracture and degenerative joint disease.²⁶⁻²⁸ Although associated imaging findings may be incidental, pathology of the equine cervical APJs can also result in cervical nerve root and spinal cord compression leading to clinical signs such as decreased cervical ROM, lameness and ataxia.^{16,23,27,29-32} Pathology in the equine cervical spine commonly involves a dynamic component. Therefore, assessment of affected segments in motion has the potential to aid the detection of dynamic stenotic conditions.

The aim of this study was to investigate the feasibility of dynamic CT for diagnostic imaging of the equine cervical APJs and to give a detailed description of APJ movement in a cadaver model. We hypothesised that dynamic CT facilitates the comprehensive assessment of the equine cervical APJ components in motion.

2 | MATERIALS AND METHODS

2.1 | Neck specimens

Cervical specimens ($n = 12$) were collected from Warmblood horses without evidence of cervical pathology, humanely destroyed for reasons unrelated to this study. Horses were between 3 and 31 years of age (mean = 12 years) and included six geldings and six mares. This sampling protocol was adopted to comply with the exploratory nature of this study and with animal welfare considerations.

Specimens were excised at the atlantooccipital joint and at the cervicothoracic junction.²⁴ The perivertebral musculature including the intertransversarii cervicis and longus colli muscles and the joint capsules were left intact. Specimens were frozen at -20°C immediately after dissection and subsequently thawed over 24 hours at 10°C prior to biomechanical testing.

2.2 | Testing device

Based on a previous protocol, a custom-made motorised testing device was used to position and manipulate the neck specimens to perform dynamic computed tomographic (dynamic 2D and 3D CT) imaging (Figure 1).²⁴ The testing device provided consistent and controlled movement of the APJ

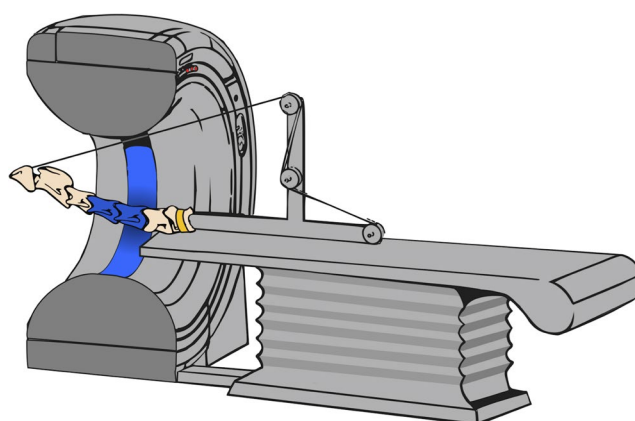


FIGURE 1 Custom-made motorised device for biomechanical testing of equine neck specimens (C_1 - C_7). A specimen is illustrated in neutral position for computed tomographic (CT) imaging (320-detector-row CT scanner, Aquilion One, Canon Medical Systems) of the motion segment $C_{4/5}$ (field of view indicated in blue). The body of C_7 is fixed in the device (yellow band). C_1 is secured to a rope, leading through a pulley system and attached to a rope winch

in flexion and extension. The vertebral body of C_7 was fixed in the device and C_1 was attached to a rope which led through a pulley and was connected to a rope winch. Additionally, a wooden frame was used to support the weight of the specimen during motion. The motion segment $C_{4/5}$ was evaluated in this study. The two motion segments ($C_{5/6}$ and $C_{6/7}$) caudal to the motion segment of interest ($C_{4/5}$) were not attached to the frame, to allow full ROM of these adjacent segments. The applied force was standardised and limited to 50 Nm and the speed to 0.05 m/seconds.³³

2.3 | Computed tomographic imaging

Computed tomographic imaging was performed using an intermittent sequential mode with a 320 detector row CT scanner with a 160 mm wide-area (2D) solid-state detector design that allows image acquisition of a volumetric axial length of 160 mm without moving the CT couch (Aquilion One; Canon Medical Systems). The gantry opening was 78 cm. A field-of-view of 50 cm with 512×512 pixels, 0.5 mm slice thickness and a tube rotation time of 0.35 seconds at 100 kVp and 280 mAs (100 effective mAs) were used. Supplementary videos illustrate the CT data (Videos S1-S4): Two dynamic CT scans including full range of extension (Video S1) and flexion (Video S3) and were performed on each neck specimen with focus on the motion segment $C_{4/5}$.

2.4 | Computed tomography analysis

The movement of each cervical spine segment ($C_{4/5}$) was viewed in three planes using multiplanar reconstruction (MPR) mode (dynamic 2D

CT) (Figure 2). Sagittal plane images were exported as 2D videos (Videos S1 and S3) as well as dynamic 3D reconstructions (volume rendering) (Videos S2 and S4 and Figure 3). Prior to further evaluation, images were screened for the presence of pathological changes and specimens with evidence of cervical spine pathology were not included in the trial.

For the assessment of the overall image quality and presence of motion artefacts, the dynamic 2D and dynamic 3D videos were divided into four phases of movement. Phases were equally long, with 2-4 seconds per phase depending on the total length of the motion cycle (maximum length 14 seconds). A subjective scale of 1-4 (1 = excellent, no motion artefacts; 2 = good, subtle motion artefacts; 3 = fair, moderate motion artefacts, evaluation possible and 4 = poor, severe motion artefacts, evaluation not possible) was used to grade the overall image quality in each of the four phases (Figure 4). The overall image quality of all four phases was additionally evaluated based on the same score.

Images were blinded and analysed independently by a board-certified veterinary radiologist (KV), a board-certified veterinary surgeon (AE) and a third-year equine surgery resident (NS) using open-source imaging software with three-dimensional multiplanar reconstruction (MPR) capability (Horos 64-bit DICOM viewer, Horos Project, 2015) on an image analysis workstation (Apple iMac Pro 2017). The sum of scores attributed by each observer for each of the four phases of movement was used to assess the intra- and inter-observer agreement. The intra-observer agreement was determined by evaluating all images twice within one month (NS) and the evaluation of the inter-observer agreement was based on a comparison of the three observers (KV, AE, NS).

For the analysis of the APJ movement pattern, three images were selected for each $C_{4/5}$ motion segment, one with the cervical spine in a neutral position, one in maximal flexion and one in maximal

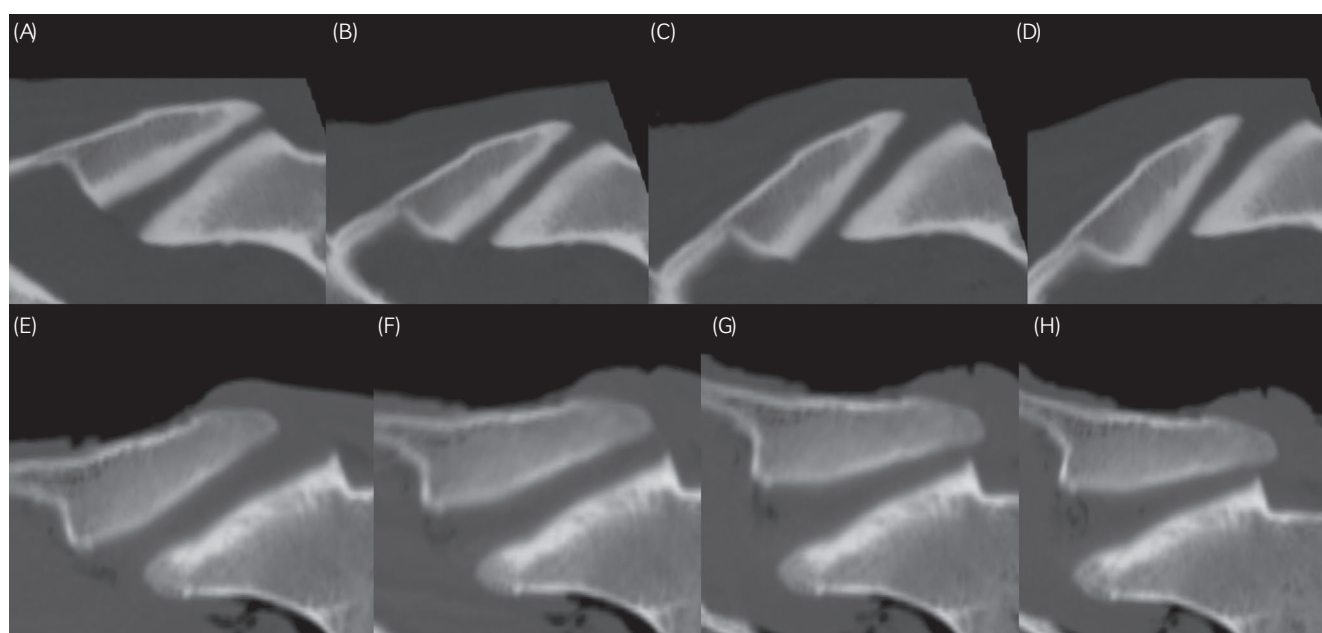


FIGURE 2 Following computer tomographic evaluation, dynamic 2D sagittal plane videos of the $C_{4/5}$ motion segment were divided into four phases of movement. Starting at the neutral position (A), 2D captures of initial (B), mid- (C) and full-flexion (D) as well as neutral position (E) initial (F), mid- (G) and full-extension (H) are shown. The four phases of each motion cycle were assessed for overall image quality and presence of motion artefacts

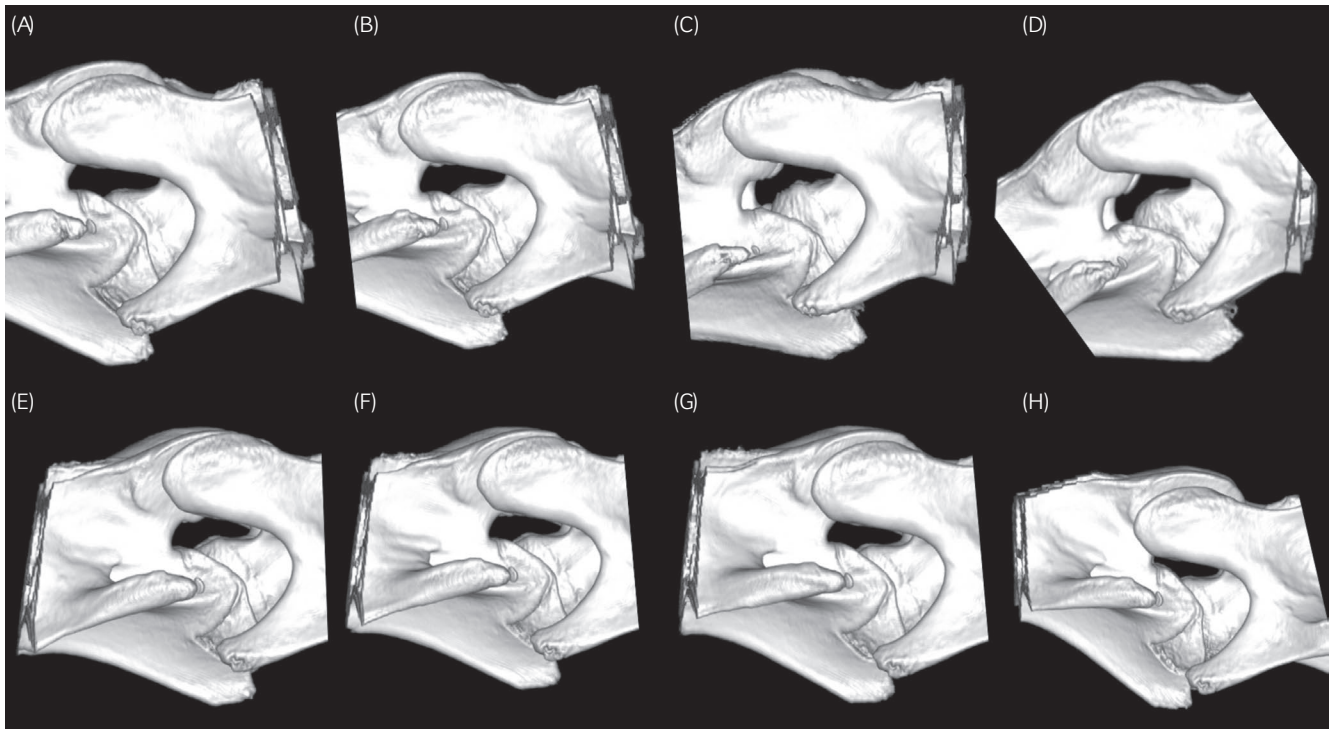


FIGURE 3 Sagittal plane computer tomographic images were exported as dynamic 3D reconstructions (volume rendering). The dynamic 3D videos of the $C_{4/5}$ motion segment were split into four phases of flexion (A-D) and extension (E-H) movement and graded to describe the presence of motion artefacts and the image quality

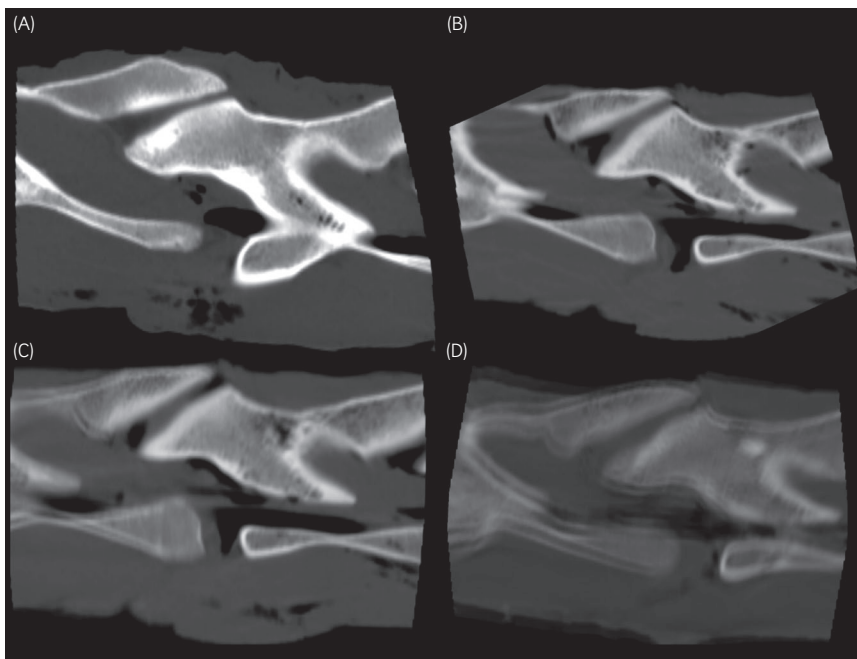


FIGURE 4 Four phases of a movement cycle (flexion and extension) were assessed based on video sequences (2D and 3D) of the dynamic computer tomographic evaluation of the $C_{4/5}$ motion segment of 12 equine cervical spine specimens. The presence of motion artefacts and the overall image quality were subjectively graded as 1 = excellent, no motion artefacts (A); 2 = good, subtle motion artefacts (B); 3 = fair, moderate motion artefacts, evaluation possible (C) and 4 = poor, severe motion artefacts, evaluation not possible (D) by three-blinded observers

extension. The neutral position was defined as the point at which the caudal aspect of the cranial articular process of C_5 and the caudal aspect of the caudal articular process of C_4 were superimposed. In flexion, the cranial translational displacement of the caudal articular process of C_4 relative to the cranial articular process of C_5 was measured. In extension, the caudal translational displacement of the caudal articular process of C_4 compared with the cranial articular process of C_5 was determined (Figure 5).

2.5 | Data analysis

Data were recorded in Excel (Microsoft Inc) and analysed in SPSS (IBM® SPSS® Statistics). Data were visually assessed and found not to be normally distributed and analysed using the Wilcoxon signed-rank test for pairwise comparison to compare the difference of translation in flexion vs. extension movements and the difference between the right and left translations both in flexion and extension

movements. The intra-observer agreement was assessed using the Wilcoxon Signed Rank Test and the inter-observer agreement was determined using the Friedman test. For all tests, a P -value of $<.05$ was considered statistically significant. A Bonferroni correction was applied to the significance threshold when relevant.

3 | RESULTS

3.1 | Dynamic 2D image quality and artefacts

In flexion, the median image quality of the dynamic 2D imaging was rated with a score of 2 (95% CI: 1-3) in phase II. Subtle motion artefacts were visible but did not impact on the image evaluation. Flexion phases I, III and IV (95% CI: 1-3.05, 1-3 and 1-1.05, respectively) were graded with a score of 1 without evidence for motion artefacts. In extension, the median image quality was graded with an average score of 1.5 in phases I and II (95% CI: 1-3.05 both). Phases III and IV were rated with 1 (95% CI: 1-2.05 and 1-2, respectively). The median overall image quality of all four phases was 1 in flexion and extension (95% CI: 1-3 both).

3.2 | Dynamic 3D image quality and artefacts

For the dynamic 3D videos, all raters gave excellent scores (1) for phases I-IV in flexion and extension. The median overall image quality of all four phases was also rated as 1 in flexion and extension.

3.3 | Dynamic 2D vs. dynamic 3D image quality

The image quality of the dynamic 3D videos was significantly better when compared with the dynamic 2D videos in flexion and

extension. A significantly lower score was observed in the dynamic 3D videos over the four phases by the three observers for both flexion (95% CI: 1-2 and 1-3, respectively for 3D and 2D videos; $P = .007$) and extension movement (95% CI: 1-2 and 1-3, respectively for 3D and 2D videos; $P = .008$).

3.4 | Intra- and interobserver agreement

No significant intra-observer difference (dynamic 2D flexion 95% CI: 4-7.73 vs 4.28-8, $P = .8$; dynamic 2D extension 95% CI: 4-9.5 vs 4-9.7, $P = .4$; dynamic 3D flexion 95% CI: 4-6 vs 4-6, $P = 1$; dynamic 3D extension 95% CI: 4-5 vs 4-5.73, $P = .4$) was detected between the two summed scores attributed by the same observer (NS) for the studied movements (flexion and extension) in both 2D and 3D videos at different time points. A significant inter-observer difference was evident between the summed scores given by the three observers for the 2D videos for both the flexion (95% CI: 4-7.73, 4-8.73 and 4-6.73, respectively, for the three observers, $P = .001$) and extension (95% CI: 4-9.45, 4-9.9 and 4-6.73, respectively, for the three observers, $P = .009$) movement. Good inter-observer agreement was found for the assessment of dynamic 3D videos for flexion (95% CI: 4-6, 4-6 and 4-5.73, respectively, for the three observers, $P = .9$) and extension (95% CI: 4-5, 4-7.45 and 4-6, respectively, for the three observers, $P = .6$).

3.5 | Translational displacement of the APJ surfaces

The median length of the cranial and caudal APJ surface was 43.57 mm. In flexion, the median displacement of the caudal APJ surface of C_4 relative to the cranial APJ surface of C_5 was 18.79 mm towards cranial for the left side and 17.22 mm for the right side

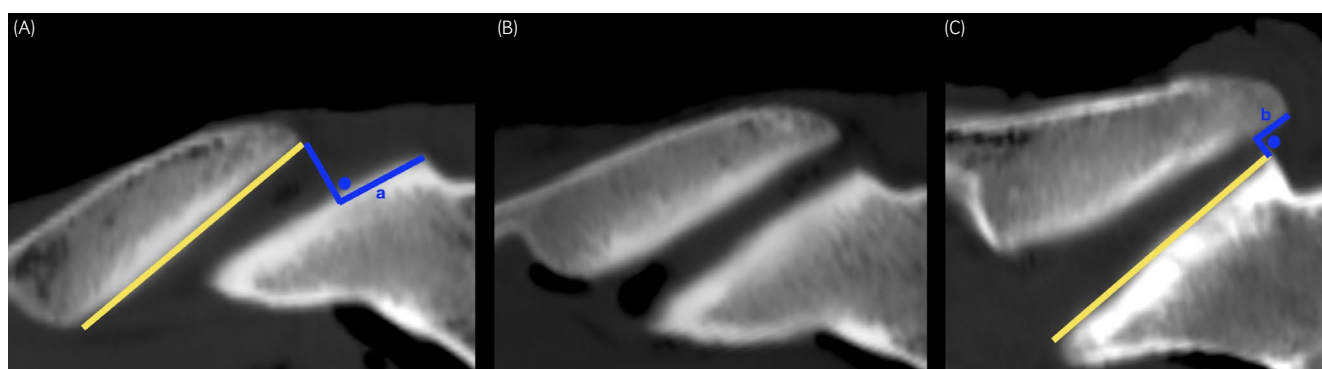


FIGURE 5 (A) Two-dimensional sagittal plane computer tomographic (CT) image of $C_{4/5}$ in maximal flexion. The translational displacement of the caudal articular process joint (APJ) surface of C_4 against the cranial APJ surface of C_5 towards cranial was measured as indicated. yellow line = length of the caudal APJ surface of C_4 ; blue right angle = translational displacement in flexion (a). (B) Two-dimensional sagittal plane CT image of $C_{4/5}$ in neutral position with the caudal aspect of the APJ surface of C_4 and C_5 superimposed. (C) Two-dimensional sagittal plane CT image of $C_{4/5}$ in maximal extension. The translational displacement of the caudal APJ surface of C_4 against the cranial APJ surface of C_5 towards caudal was determined as shown. yellow line = length of the cranial APJ surface of C_5 ; blue right angle = translational displacement in extension (b)

(Figure 5A). In extension, the median displacement of the caudal APJ surface of C₄ relative to the cranial APJ surface of C₅ was 2.78 mm towards caudal for the left side and 1.82 mm for the right side (Figure 5C). There was no statistically significant difference in the displacement of the APJs between the left and right sides of the flexion (95% CI: 12.78-23.00 and 12.00-21.87, respectively, for left and right sides; $P = .5$) and extension (95% CI: 1.21-6.04 and 0-8.26, respectively for left and right sides; $P = .3$) However, significantly more translational displacement was evident in flexion when compared with extension ($P = .002$ for both the right and the left sides).

4 | DISCUSSION

The results of this study confirm the feasibility of dynamic 2D and 3D CT for the assessment of the equine cervical APJs based on a cadaver model. Additionally, the investigation gives new insight in the dynamics of the APJ articular components during motion.

Blinded evaluation of 2D and 3D video sequences derived from sagittal plane CT data focused on the motion segment C_{4/5} identified an excellent overall image quality for both, flexion and extension movement. During dynamic 2D CT imaging, there was evidence of slight motion artefacts adjacent to the APJs in movement phases I and II in flexion and extension. Most artefacts were observed in the vicinity of the APJs as the soft tissues showed a higher velocity of movement than the APJs themselves. Whilst motion artefacts can impair on image analysis and post-processing, it has been demonstrated that the assessment of axial CT sequences is not qualitatively affected by object motion at 0.05 m/seconds.² In addition, each dynamic CT study consists of multiple individual axial sequences, at least one of which was always free of motion artefacts and could be used diagnostically for multiplanar reconstruction without restriction.

The volume acquisition speed of the CT is the most important parameter for motion artefact control.³⁴ The volume acquisition speed depends on the gantry rotation speed and the image reconstruction technique.³⁵ An exponential decrease in image quality was seen with lower volume acquisition speeds in previous studies.^{2,36} Based on these results the highest gantry rotation speed (0.32 seconds per rotation) is recommended when performing dynamic CT examination.^{2,36} The speed of motion of the biomechanical testing device further influences the development of motion artefacts.¹¹ The speed of the vertebral flexion and extension was pre-determined at 0.05 m/seconds.²⁴ Most likely a slower speed would have resulted in an improved image quality, but also a substantially higher amount of image data as each acquired volume (0.32 seconds) contains 516 images.³⁷

The dynamic 3D videos were free of motion artefacts in phases I-IV in flexion and extension in the current study. This observation can be explained by the calculation of the 3D volume from axial 2D slices, which is accompanied by a loss of resolution. In contrast to another study, there was no evidence for band artefacts in the dataset presented here.³⁸ The wider detector of the CT used (320

detector - row with 160 mm detector width) might mitigate this type of artefact.

Good intra-observer agreement was found for the assessment of dynamic 2D and 3D videos; however, inter-observer agreement was only evident for dynamic 3D but not dynamic 2D video evaluation. This finding is most likely related to the motion artefacts seen in phases I and II of the 2D videos being very subtle.

The dynamic CT data was used to further investigate the detailed movement pattern of the equine cervical APJs. The translational displacement of the APJ articular surfaces was significantly greater in flexion when compared with extension. In flexion, there was a mean displacement of the APJ surface of over 43% in relation to the mean length of the APJ surface with a displacement of only approximately 7% observed during cervical extension. The exact aetiopathogenesis of cervical APJ osteoarthritis and osteochondrosis is yet to be determined.³⁹⁻⁴¹ Analysis of the dynamic 2D video series of the C_{4/5} APJ identified that the cranial margin of C₅ was located in close proximity to the C₄ articular surface in full flexion. Similarly, the caudal margin of C₅ showed what could be interpreted as an area of increased pressure or impingement on the articular surface of C₄ in full extension of the cervical spine, potentially contributing to the development of osteochondrosis or osteoarthritis in this area (Figure 6). In a recent report, osteochondral fragments were identified in 24% of horses with cervical dysfunction.¹⁹ The majority of fragments (19/22) were located within the APJ synovial outpouchings, in either a ventral axial or dorsal abaxial location adjacent to the articular margin.

Besides the described musculoskeletal applications, dynamic CT facilitates radiotherapy planning in human patients.³⁷ Targeted radiation can be performed in cases with thoracic neoplasia resulting in a reduced chance of a geographic miss due to movement artefacts.^{37,42} Dynamic CT angiography is used for visualisation of vascular pathology in the brain and spine and contrast agent enhancement in the heart and pulmonary vessels can be displayed in real time during a cardiac cycle.^{37,43,44}

Static CT is an accepted modality in equine orthopaedic advanced diagnostic imaging and an excellent tool for the evaluation of fracture configurations in equine patients.^{1,45-47} The ability to display the interaction of articular components during complex movements using dynamic CT additionally facilitates the investigation of potential mechanisms of joint injury. Wide area-detector CT scanners are particularly useful for dynamic studies as they provide high temporal resolution and whole-joint coverage during sequential acquisition.⁷ Challenges with the widespread use of dynamic CT in routine diagnostic imaging include the cost of the scanner as well as handling and processing of the large volumetric datasets that are generated using this technique.³⁷

In human medicine, the patient is fully conscious and actively performs controlled movements during dynamic CT examination. In veterinary patients, sedation or general anaesthesia is required in order to image controlled movement patterns. In the described investigation, constant and continuous movement of the spinal motion segment C_{4/5} was achieved with the aid of a motor-driven external device.²⁴ Whilst the application of dynamic CT remains technically more demanding

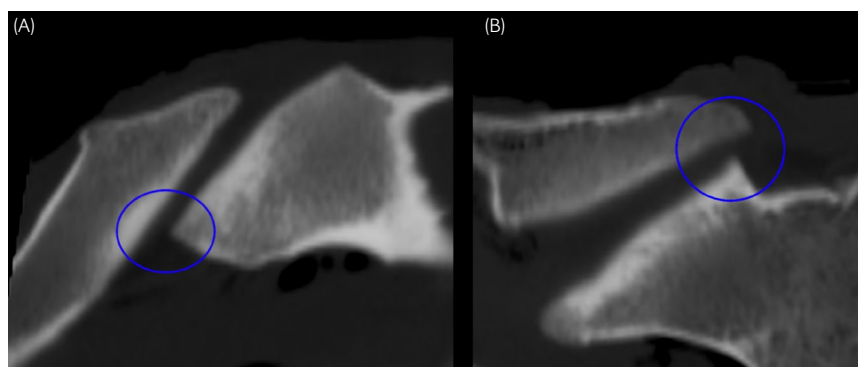


FIGURE 6 (A) Two-dimensional sagittal plane computer tomographic (CT) image of $C_{4/5}$ in maximal flexion. Note the close position of the cranial aspect of the cranial articular process of C_5 in relation to the caudal C_4 articular process joint (APJ) surface (blue circle). (B) Two-dimensional sagittal plane CT image of $C_{4/5}$ in maximal extension. Focused pressure on the caudal margin of the C_5 articular process in this position (blue circle) could relate to an additional predilection site for APJ osteochondrosis and osteoarthritis

in horses when compared with human or small animal patients, the development of similar devices might be useful for the assessment of other regions of the body including the equine distal limb. In humans, however, this CT shows its strength primarily in examinations of anatomical structures in which motion artefacts cannot be avoided (heart and lungs).³⁷ Recently, the possibility of examining limbs of the standing horse (without general anaesthesia) with high-end fan-beam CT systems was introduced.⁴⁸ Since a distal limb of a standing horse can be examined in 0.32 seconds with this system, significantly less influence of motion artefacts can be expected.

Limitations of the described study are the *ex vivo* protocol used and the small number of specimens included. Based on previously described protocols, spines were excised at the level of the atlantooccipital and the cervicothoracic junction with only the perivertebral musculature and the joint capsules left intact.^{23,49} Excision might have influenced the mobility of the spine when compared with the ROM of the equine cervical spine in its entirety. Fixation of the cervical spine specimens in the testing device could have additionally impaired on the motion of the APJs. The motion segments adjacent to $C_{4/5}$ were not attached to the frame to minimise the impact of the construct on the cervical ROM.

The described findings should be interpreted carefully with regard to the exploratory nature of the study. The relatively small sample size and the not randomly selected investigated sample may influence results where non-significant differences were found. Additionally, it may not be valid to draw direct conclusions from the data concerning $C_{4/5}$ and apply it to other motion segments in the cervical spine as differences in ROM are known to exist particularly towards the cranial cervical spine (C_1 - C_3). However, the study is a first step to show the potential of dynamic 3D CT in veterinary medicine.

In conclusion, the results of this study confirm that a CT with a detector coverage of 16 cm and a rotation speed of 0.32 seconds makes it possible to obtain high-quality images of equine cervical articular process joint $C_{4/5}$ in motion. As the acquired dynamic data sets consist of multiple individual volume sets, slight motion artefacts in individual video sequences can be replaced by a different volume for the evaluation of stationary (2D) images. This work further confirms

that dynamic CT imaging has the potential to provide new insight into the movement pattern of articular motion segments, which may be of value for the examination of APJ and other joint conditions. The study provides a first step in the investigation of the potential of dynamic 3D CT in veterinary medicine, a technique that has only begun to be explored and leaves much room for refinement prior to its introduction in routine practice.

ACKNOWLEDGEMENTS

We thank the Leibniz Institute for Zoo and Wildlife Research and gratefully acknowledge Alexander Gernhardt for his assistance with the biomechanical testing device and Carola Giersch for 3D illustration of the device. Open access funding enabled and organized by ProjektDEAL.

CONFLICT OF INTERESTS

No competing interests have been declared.

AUTHOR CONTRIBUTIONS

All authors contributed to the study design and interpretation of the data. N. Schulze, A. Ehrle and N. Werpy were mainly responsible for the planning of the project as well as data acquisition, analysis and interpretation. G. Fritsch, R. Klopffleisch, J. Gernhard, C. Lischer and T. Hildebrandt contributed to the study execution and data analysis. K. Vanderperren and N. Werpy developed the described image analysis and R. Ben Romdhane was mainly responsible for data acquisition and statistical analysis. All authors approved the final version of the manuscript.

ETHICAL ANIMAL RESEARCH

Approval for the study was given by the local Committee on Research Ethics.

INFORMED CONSENT

Explicit owner informed consent for this study was not obtained but horse owners were made aware that tissues would be used for research in general.

PEER REVIEW

The peer review history for this article is available at <https://publons.com/publon/10.1111/evj.13560>.

DATA AVAILABILITY STATEMENT

The data that support the findings of this study are available from the corresponding author upon reasonable request.

ORCID

Nicole Schulze  <https://orcid.org/0000-0002-1304-5190>

Robert Klopffleisch  <https://orcid.org/0000-0002-6308-0568>

Racem Ben Romdhane  <https://orcid.org/0000-0001-8783-7775>

Anna Ehrle  <https://orcid.org/0000-0001-5338-6195>

REFERENCES

- Preux M, Klopffleisch R, Bregger MD, Brünisholz HP, Van der Vekens E, Schweizer-Gorgas D, Koch C, et al. Clinical use of computer-assisted orthopedic surgery in horses. *Vet Surg*. 2020;49:1075–87.
- Gondim Teixeira PA, Formery A-S, Hossu G, Winninger D, Batch T, Gervaise A, et al. Evidence-based recommendations for musculoskeletal kinematic 4D-CT studies using wide area-detector scanners: a phantom study with cadaveric correlation. *Eur Radiol*. 2017;27:437–46.
- Kerkhof FD, Brugman E, D'Agostino P, Dourthe B, van Lenthe GH, Stockmans F, et al. Quantifying thumb opposition kinematics using dynamic computed tomography. *J Biomech*. 2016;49:1994–9.
- White J, Couzens G, Jeffery C. The use of 4D-CT in assessing wrist kinematics and pathology. *Bone Joint J*. 2019;101-B(11):1325–1330.
- Alta TD, Bell SN, Troupis JM, Coghlan JA, Miller D, et al. The new 4-dimensional computed tomographic scanner allows dynamic visualization and measurement of normal acromioclavicular joint motion in an unloaded and loaded condition. *J Comput Assist Tomogr*. 2012;36:749–54.
- Choi YS, Lee YH, Kim S, Cho HW, Song H-T, Suh J-S, et al. Four-dimensional real-time cine images of wrist joint kinematics using dual source CT with minimal time increment scanning. *Yonsei Med J*. 2013;54:1026–32.
- Gondim Teixeira PA, Gervaise A, Louis M, Lecocq S, Raymond A, Aptel S, et al. Musculoskeletal wide detector CT: principles, techniques and applications in clinical practice and research. *Eur J Radiol*. 2015;84:892–900.
- Leng S, Zhao K, Qu M, An K-N, Berger R, McCollough CH, et al. Dynamic CT technique for assessment of wrist joint instabilities. *Med Phys*. 2011;38(Suppl 1):S50.
- Edirisinghe Y, Troupis JM, Patel M, Smith J, Crossett M. Dynamic motion analysis of dart throwers motion visualized through computerized tomography and calculation of the axis of rotation. *J Hand Surg Eur*. 2014;39:364–72.
- Shapeero LG, Dye SF, Lipton MJ, Gould RG, Galvin EG, Genant HK, et al. Functional dynamics of the knee joint by ultrafast, cine-CT. *Invest Radiol*. 1988;23:118–23.
- Tay S-C, Primak AN, Fletcher JG, Schmidt B, Amrami KK, Berger RA, et al. Four-dimensional computed tomographic imaging in the wrist: proof of feasibility in a cadaveric model. *Skeletal Radiol*. 2007;36:1163–9.
- Totterman S, Tamez-Pena J, Kwok E, Strang J, Smith J, Rubens D, et al. 3D visual presentation of shoulder joint motion. *Stud Health Technol Inform*. 1998;50:27–33.
- Wassilew GI, Janz V, Heller MO, Tohtz S, Rogalla P, Hein P, et al. Real time visualization of femoroacetabular impingement and subluxation using 320-slice computed tomography. *J Orthop Res*. 2013;31:275–81.
- Bergmann W, Mik-van Mourik M, Veraa S, Broek J, Wijnberg ID, Back W, et al. Cervical articular process joint osteochondrosis in Warmblood foals. *Equine Vet J*. 2020;52:664–9.
- Dyson SJ. Unexplained forelimb lameness possibly associated with radiculopathy. *Equine Vet Educ*. 2020;32(S10):92–103.
- García-López JM. Neck, back, and pelvic pain in sport horses. *Vet Clin North Am Equine Pract*. 2018;34:235–51.
- Pérez-Nogués M, Vaughan B, Phillips KL, Galuppo LD. Evaluation of the caudal cervical articular process joints by using a needle arthroscope in standing horses. *Vet Surg*. 2020;49:463–71.
- Thomsen LN, Berg LC, Markussen B, Thomsen PD. Synovial folds in equine articular process joints. *Equine Vet J*. 2013;45:448–53.
- Tucker R, Hall YS, Hughes TK, Parker RA. Osteochondral fragmentation of the cervical articular process joints; prevalence in horses undergoing CT for investigation of cervical dysfunction. *Equine Vet J*. 2020;54:106–13. <https://doi.org/10.1111/evj.13410>
- Puchalski SM. Advances in equine computed tomography and use of contrast media. *Vet Clin North Am Equine Pract*. 2012;28:563–81.
- Wright L, Puchalski SM, Kristoffersen M, Lindegaard C. Arthroscopic approach and intra-articular anatomy of the equine atlanto-occipital joint. *Vet Surg*. 2018;47:756–67.
- Lindgren CM, Wright L, Kristoffersen M, Puchalski SM. Computed tomography and myelography of the equine cervical spine: 180 cases (2013–2018). *Equine Vet Educ*. 2021;33(9):475–83. <http://dx.doi.org/10.1111/eve.13350>
- Clayton HM, Townsend HG. Kinematics of the cervical spine of the adult horse. *Equine Vet J*. 1989;21:189–92.
- Schulze N, Ehrle A, Weller R, Fritsch G, Gernhardt J, Ben Romdhane R, et al. Computed tomographic evaluation of adjacent segment motion after ex vivo fusion of equine third and fourth cervical vertebrae. *Vet Comp Orthop Traumatol*. 2020;33:1–8.
- Zsoldos RR, Licka TF. The equine neck and its function during movement and locomotion. *Zoology (Jena)*. 2015;118:364–76.
- Pool RR. Difficulties in definition of equine osteochondrosis; differentiation of developmental and acquired lesions. *Equine Vet J*. 1993;25:5–12.
- Powers BE, Stashak TS, Nixon AJ, Yovich JV, Norrdin RW. Pathology of the vertebral column of horses with cervical static stenosis. *Vet Pathol*. 1986;23:392–9.
- Rooney JR. Osteochondrosis in the horse. *Mod Vet Pract*. 1975;56:41–3.
- Dyson SJ. Lesions of the equine neck resulting in lameness or poor performance. *Vet Clin North Am Equine Pract*. 2011;27:417–37.
- Ricardi G, Dyson SJ. Forelimb lameness associated with radiographic abnormalities of the cervical vertebrae. *Equine Vet J*. 1993;25:422–6.
- Stewart RH, Reed SM, Weisbrode SE. Frequency and severity of osteochondrosis in horses with cervical stenotic myelopathy. *Am J Vet Res*. 1991;52:873–9.
- Trostle SS, Dubielzig RR, Beck KA. Examination of frozen cross sections of cervical spinal intersegments in nine horses with cervical vertebral malformation: lesions associated with spinal cord compression. *J Vet Diagn Invest*. 1993;5:423–31.
- Gellman K, Bertram J. The equine nuchal ligament 2: passive dynamic energy exchange in locomotion. *Vet Comp Orthop Traumatol*. 2002;15:7–14.
- Grosjean R, Sauer B, Guerra RM, Blum A, Felblinger J, Hubert J. Degradation of the z-resolution due to a longitudinal motion with a 64-channel CT scanner. *Annu Int Conf IEEE Eng Med Biol Soc*. 2007;2007:4429–32.
- Beeres M, Wichmann JL, Paul J, Mbalisike E, Elsabaie M, Vogl TJ, et al. CT chest and gantry rotation time: does the rotation time influence image quality? *Acta Radiol*. 2015;56:950–4.
- Dawson P, Lees WR. Multi-slice technology in computed tomography. *Clin Radiol*. 2001;56:302–9.

37. Kwong Y, Mel AO, Wheeler G, Troupis JM. Four-dimensional computed tomography (4DCT): a review of the current status and applications. *J Med Imaging Radiat Oncol.* 2015;59:545–54.
38. Taguchi K, Chiang BS, Hein IA. Direct cone-beam cardiac reconstruction algorithm with cardiac banding artifact correction. *Med Phys.* 2006;33:521–39.
39. DeRouen A, Spriet M, Aleman M. Prevalence of anatomical variation of the sixth cervical vertebra and association with vertebral canal stenosis and articular process osteoarthritis in the horses. *Vet Radiol Ultrasound.* 2016;57:253–8.
40. Birmingham SSW, Reed SM, Mattoon JS, Saville WJ. Qualitative assessment of corticosteroid cervical articular facet injection in symptomatic horses. *Equine Vet Educ.* 2010;22:77–82.
41. Pepe M, Angelone M, Gialletti R, Nannarone S, Beccati F. Arthroscopic anatomy of the equine cervical articular process joints. *Equine Vet J.* 2014;46:345–51.
42. Wang LU, Hayes S, Paskalev K, Jin L, Buyyounouski MK, Ma C-M, et al. Dosimetric comparison of stereotactic body radiotherapy using 4D CT and multiphase CT images for treatment planning of lung cancer: evaluation of the impact on daily dose coverage. *Radiother Oncol.* 2009;91:314–24.
43. Numata S, Tsutsumi Y, Monta O, Yamazaki S, Seo H, Yoshida S, et al. Mechanical valve evaluation with four-dimensional computed tomography. *J Heart Valve Dis.* 2013;22:837–42.
44. Suzuki K, Morita S, Masukawa AI, Machida H, Ueno E. Diagnosing a large slowly enhanced cerebral aneurysm using four-dimensional multiphase dynamic contrast-enhanced computed tomography angiography. *Jpn J Radiol.* 2010;28:680–3.
45. Gasiorowski JC, Richardson DW. Clinical use of computed tomography and surface markers to assist internal fixation within the equine hoof. *Vet Surg.* 2015;44:214–22.
46. Puchalski SM, Galuppo LD, Hornof WJ, Wisner ER. Intraarterial contrast-enhanced computed tomography of the equine distal extremity. *Vet Radiol Ultrasound.* 2007;48:21–9.
47. Jackson MA, Ohlerth S, Fürst AE. Use of an aiming device and computed tomography for assisted debridement of subchondral cystic lesions in the limbs of horses. *Vet Surg.* 2019;48:O15–24.
48. Mageed M. Standing computed tomography of the equine limb using a multi-slice helical scanner: technique and feasibility study. *Equine Vet Educ.* 2021;34(2):77–83. <https://doi.org/10.1111/eve.13388>
49. Sleutjens J, Cooley AJ, Sampson SN, Wijnberg ID, Back W, van der Kolk JH, et al. The equine cervical spine: comparing MRI and contrast-enhanced CT images with anatomic slices in the sagittal, dorsal, and transverse plane. *Vet Q.* 2014;34:74–84.

SUPPORTING INFORMATION

Additional supporting information may be found in the online version of the article at the publisher's website.

How to cite this article: Schulze N, Werpy N, Gernhardt J, Fritsch G, Hildebrandt T, Vanderperren K, et al. Dynamic three-dimensional computed tomographic imaging facilitates evaluation of the equine cervical articular process joint in motion. *Equine Vet J.* 2022;00:1–9. doi:[10.1111/evj.13560](https://doi.org/10.1111/evj.13560)

3.3 Internal fixation of a complete ventral luxation of the dens axis in an American quarter horse yearling

Authors: Nicole Schulze; Anna Ehrle; Andrea C. Noguera Cender; Christoph J. Lischer;

Publication: Equine Veterinary Surgery 2019 Nov;48(8):1500-1506.

DOI: 10.1111/vsu.13283

Correspondence Address:

Dr. med. vet. Nicole Schulze

Klinik für Pferde

Fachbereich Veterinärmedizin

Freie Universität Berlin, Oertzenweg 19B, 14163 Berlin

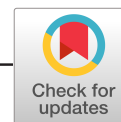
Phone: +49 30 838 622 99

Fax: +49 30 838 625 29

Email: nicole.schulze@fu-berlin.de

Authorship: All authors contributed to the study design and interpretation of the data.

All authors approved the final version of the manuscript.



CASE REPORT

WILEY

Internal fixation of a complete ventral luxation of the dens axis in an American quarter horse yearling

Nicole Schulze DVM | Anna Ehrle DVM Diplomate ECVS |

Andrea C. Noguera Cender DVM Diplomate ECVS | Christoph Lischer DVM Dipolmate ECVS

Equine Clinic, Surgery, and Radiology,
Freie Universität Berlin, Berlin, Germany

Correspondence

Nicole Schulze, Equine Clinic, Surgery and
Radiology, Freie Universität Berlin,
Oertzenweg 19 b, 14163 Berlin, Germany.
Email: nicole.schulze@fu-berlin.de

Abstract

Objective: To report surgical treatment of a complete luxation of the atlantoaxial articulation with a 4.5-mm T-locking compression plate (T-LCP) in a horse.

Study design: Case report.

Animals: A one-year-old American quarter horse filly.

Methods: A one-year-old American quarter horse filly presented with a complete luxation of the atlantoaxial articulation. Closed and open reduction of the luxation were attempted under general anesthesia with the aid of a pulley system. Because the manual reduction was unsuccessful, the dens axis was excised, and the atlas and axis were stabilized with a 4.5-mm T-LCP. Four 5.5-mm cortex screws were placed across the atlantoaxial articulation in lag fashion to provide additional stability.

Results: The horse made an uneventful recovery from surgery and remained comfortable thereafter. Nine months postsurgery, the filly had developed normally and did not show any sign of ataxia or reduced mobility of the cranial neck.

Conclusion: The described surgical approach resulted in the successful stabilization of a complete luxation of the atlantoaxial articulation in an American quarter horse yearling, with a favorable outcome.

Clinical significance: Complete atlantoaxial luxation is associated with a poor prognosis for survival in horses. This is the first report of a favorable outcome after surgical stabilization. The described approach presents a valuable alternative to the manual reduction of atlantoaxial luxation in horses.

1 | INTRODUCTION

The first two vertebrae, termed *atlas* and *axis*, have a unique morphology compared with the rest of the equine cervical spine.¹ The second cervical vertebra is characterized by the dens axis, which rests in a concavity at the ventral aspect of the atlas and is held in place by several ligaments.²

Subluxation or luxation of the atlantoaxial articulation is an uncommon pathology in the horse and is seen mostly in young animals.³⁻⁵ Both conditions can be caused by congenital

defects or result from a traumatic incident.^{4,12} A complete luxation of the atlantoaxial articulation requires rupture of the apical, transverse, and alar ligaments that attached the dens axis to the atlas and occiput of the skull.^{2,4,5,9} As a consequence, the dens lies ventral to the atlantic arch, which leads to instability of the articulation and can cause spinal cord compression.⁶

In contrast to the atlantoaxial subluxation, no surgical treatment is described for the complete luxation of the articulation between the atlas and the axis.^{6,7} To the best of the authors' knowledge, this is the first report of a successful surgical

treatment of a complete luxation of the atlantoaxial articulation with a 4.5-mm T-locking compression plate (T-LCP) in a horse.

2 | CLINICAL REPORT

2.1 | History

A one-year-old American quarter horse filly was referred for further assessment of cervical trauma after a kick from another horse. The referring veterinary surgeon reported that the horse showed diffuse swelling of the cranial neck as well as pain on palpation of the cranial cervical spine. No clinical signs of ataxia were observed. Oral phenylbutazone (2.2 mg/kg) was administered, and the horse was transported to the equine referral center within 24 hours after the trauma had occurred.

2.2 | Clinical findings

At admission the horse was bright, alert, and responsive. The yearling exhibited a reduced range of motion and resented palpation of the cranial neck. Results of general clinical examination were otherwise unremarkable. Blood hematology, biochemistry, lameness, and neurological examination results were also unremarkable.

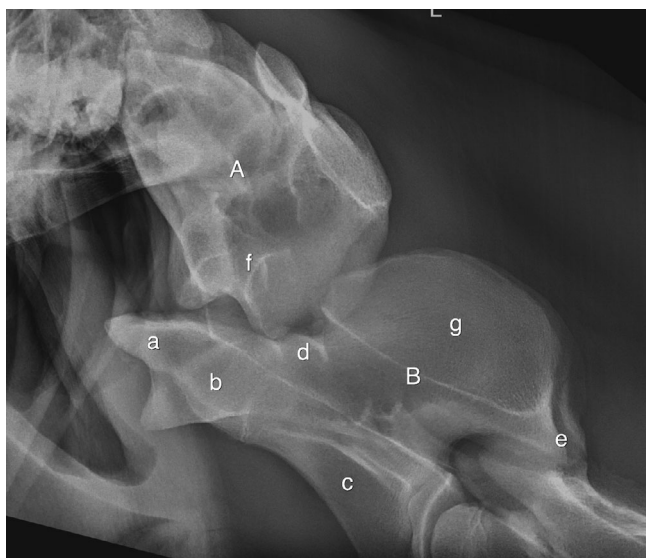


FIGURE 1 Left-lateral radiograph of a complete luxation of the dens axis in an American quarter horse yearling. The dens axis can be identified ventral to the ventral arch of the atlas. A, C₁ (atlas); B, C₂ (axis); a, dens axis; b, cranial aspect of the vertebral body of C₂; c, caudal aspect of the vertebral body of C₂; d, vertebral canal of C₂; e, articular process joint C₂/C₃; f, concavity of atlas where the dens should be located; g, dorsal spinous process of C₂

2.3 | Radiographic examination

Laterolateral and dorsoventral radiographs of the cervical spine were obtained. The radiographic examination confirmed a complete luxation of the dens axis. The atlas and axis were intact, with no evidence of an associated fracture (Figure 1).

2.4 | Surgery

Flunixin meglumine (1.1 mg/kg intravenously [IV]), amoxicillin (10 mg/kg IV), and gentamicin sulfate (6.6 mg/kg IV) were administered preoperatively. For induction of general anesthesia, the horse received medetomidine (7 µg/kg IV), diazepam (0.02 mg/kg IV), and ketamine (2.2 mg/kg IV). General anesthesia was maintained with isoflurane (minimum alveolar concentration 1.0) and xylazine (0.8 mg/kg/h IV). After induction of anesthesia, the horse was placed in dorsal recumbency with the head and neck extended. A rope was placed around the head and attached to a pulley system to apply traction to the cranial cervical spine. The reduction procedure was performed under fluoroscopic guidance (C-arm, BV Pulsera; Philips). After three unsuccessful attempts of closed manual reduction, while axial tension was applied with the pulley system, the filly was prepared for a surgical approach.

A 20-cm skin incision was made on ventral midline, centered over the atlas and axis. The musculus cutaneous colli was bluntly dissected, and the sternohyoid and sternothyroid muscles were separated in midline. After the trachea was identified, it was retracted to the left with Langenbeck retractors, and blunt dissection was continued in a dorsal direction, to the right side of the trachea. The carotid artery and vagosympathetic trunk were identified and carefully retracted by using a Penrose drain. The aponeurosis of the longus colli muscles was incised, and the muscles were retracted with Hohmann retractors to gain access to the ventral aspect of the atlas and to expose the luxated dens of the axis (Figure 2).

With the aid of the pulley system, traction was applied to the occipital area of the head of the horse in an attempt to perform open reduction of the luxation. Reduction was supported by placing a Hohmann retractor between the caudal aspect of the atlas and the dens by using it as a lever to gently walk the dens back to its physiological position. The reduction of the luxation was unsuccessful despite the application of strong traction, and the dens axis was subsequently excised with an oscillating saw (Colibri II; DePuy Synthes). The alignment of the atlas and the axis was achieved after removal of the dens axis.

The ventral spinous process of the body of the axis was flattened by using a curved osteotome and bone rongeurs. The cartilage of the caudal articular joint surface of the atlas, and the cranial articular surface of the axis was removed with a curette. The alignment of the atlas and axis was finally optimized under

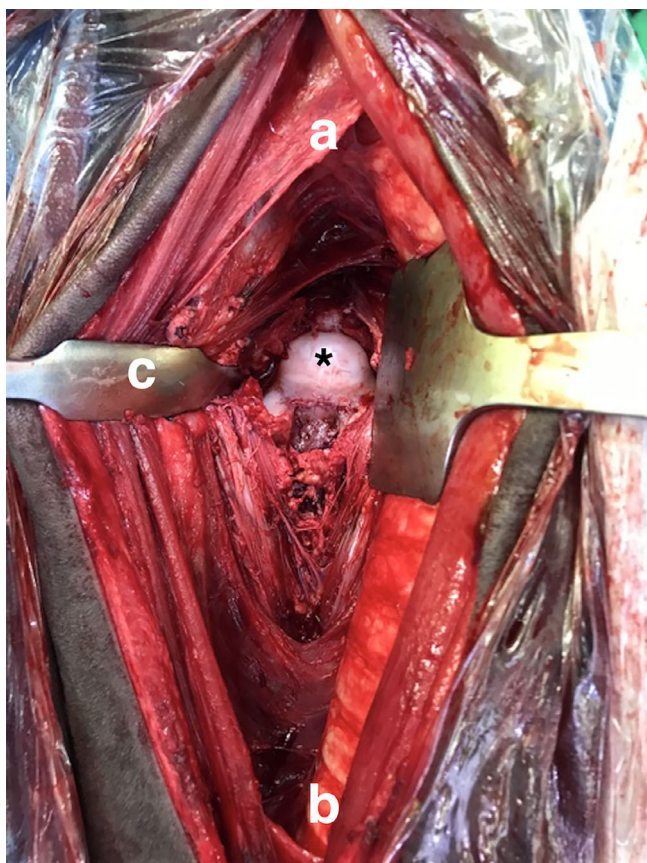


FIGURE 2 Ventral intraoperative photograph of the luxated dens of the axis. The aponeurosis of the longus colli muscles was incised, and the muscles were retracted laterally with Hohmann retractors to gain access to ventral aspect of the atlas and the axis. a, cranial; b, caudal; c, Hohmann retractor; *, luxated dens of the axis

fluoroscopic guidance and maintained with bone reduction forceps (Figure 3). A 4.5-mm six-hole T-locking compression plate (T-LCP) was contoured and fixed to the caudal aspect of the atlas with a 5-mm locking head screw (36 mm) that was inserted in the central screw hole at the T end of the plate. Care was taken not to reach the spinal canal during drilling or screw placement. The correct length of the screws was determined with fluoroscopic guidance. The second screw was a 4.5-mm cortical screw (28 mm) placed in load position in the cranial aspect of the axis (fourth screw hole). Two lateral and two medial 5.5-mm cortical screws (68 mm) were placed in lag-fashion across the articular surface of the axis and the atlas to provide additional stability. The medial and lateral cortical screws were tightened simultaneously to maintain axial alignment. The remaining screw holes of the T-LCP were filled with locking head screws with the exception of the second screw hole of the plate, which was positioned over the atlantoaxial articulation (Figure 4a,b).

Prior to closure, the wound was flushed with sterile polyionic fluids. The longus colli muscles (USP 2 polyglactin

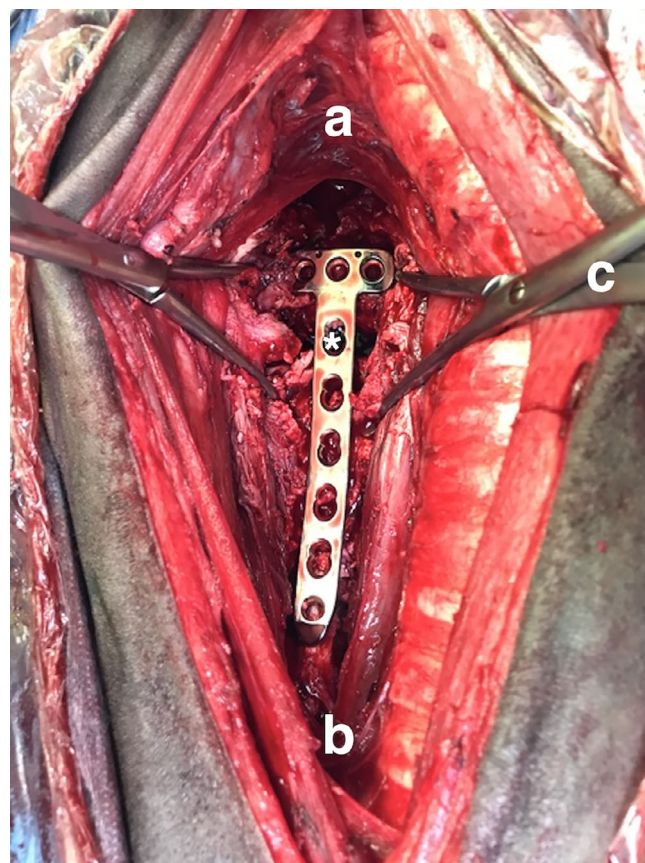


FIGURE 3 Ventral intraoperative photograph of the bone reduction forceps keeping the alignment of atlas and axis after removal of the dens axis. The ventral spinous process of the body of the axis has been flattened, and the 4.5-mm six-hole T-locking compression plate is in position. a, cranial; b, caudal; c, bone reduction forceps; *, removed dens of the axis with T-plate positioned over the atlantoaxial articulation

910), ventral cervical muscles (USP 2 polyglactin 910), cutaneous muscle together with subcutaneous tissue (USP 2-0 polyglyconate), and skin (USP 2-0 polypropylene) were apposed in simple continuous fashion. The surgical site was protected with a stent and covered with a tubular neck bandage. The hand-assisted anesthetic recovery was uneventful.

2.5 | Postoperative care

Mild wound swelling was evident postoperatively, and the animal initially displayed a reduced range of motion of the cervical spine. Hay and water were provided at shoulder height to avoid unnecessary head and neck movements. The stent was removed 2 days postoperatively, and the neck bandage was changed every 48 hours. Antimicrobial therapy was continued for 7 days (amoxicillin 10 mg/kg IV every 8 hours and gentamicin sulfate 6.6 mg/kg IV once daily),

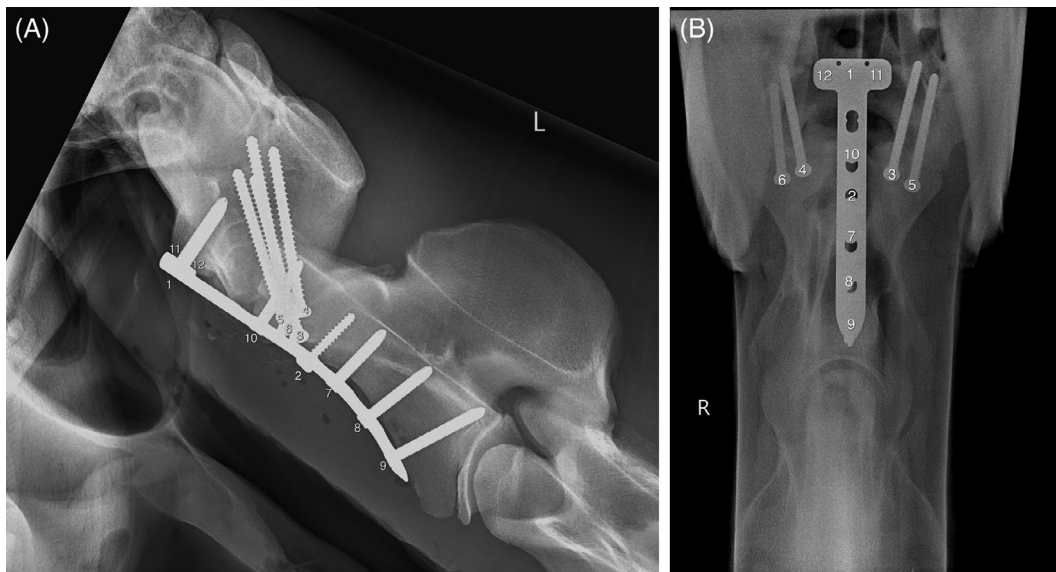


FIGURE 4 a, Left-lateral postoperative radiograph taken 3 days after surgical stabilization of a complete atlantoaxial luxation. Atlas and axis show physiological alignment, and all implants are in situ. A 4.5-mm six-hole T-locking compression plate (T-LCP) was applied to the ventral aspect of C₁ and C₂. A 5-mm locking head screw (1) was initially placed in the central hole of the T end of the plate and inserted in the ventral arch of the atlas. Then, a 4.5-mm cortical screw (2) was placed in load position in the cranial aspect of the axis. Two lateral and two medial 5.5-mm cortical screws (3-6) were inserted in lag fashion across the articular surface of the axis. The remaining screw holes (7-12) were filled with locking head screws. The second screw hole of the plate was positioned over the atlantoaxial articulation, but no screw was inserted here. Several radiolucent areas indicating gas accumulation within the esophagus and surrounding soft tissue can be noted in the area ventral to the surgical repair. b, Dorsoventral radiograph of the position of the 4.5-mm six-hole T-locking compression plate (T-LCP) and the four 5.5-mm cortical screws (3, 4, 5, 6) that were placed in lag fashion across the articular surface of the axis. Screws 3 and 4 were tightened simultaneously to maintain axial alignment. The area between C₁ and C₂ appears radiolucent because the dens axis has been excised here

and flunixin meglumine (1.1-0.5 mg/kg IV twice daily) was administered for 11 days after surgery. In addition, the horse received omeprazole (2 mg/kg once daily orally) during hospitalization.

Postoperative radiographic examination of the cervical spine was performed 3 days after surgery. All implants were in situ, and the alignment of the atlantoaxial joint was confirmed (Figure 4a,b).

Five days after surgery, the rectal temperature of the horse increased to 38.9°C, and blood hematology identified an increased white blood cell count of 12 000 cells/ μ L. A moderate increase in wound swelling and tenderness in the area of the surgical site was also observed. Results of radiographic examination did not reveal any significant findings. A moderate amount of hypochoic fluid accumulation was detected between the muscular layers of the ventral neck during ultrasonographic examination. The fluid was aspirated under ultrasonographic guidance and submitted for cytology, bacterial culture, and sensitivity testing. Based on the results of the white blood cell count (500 cells/ μ L) and the negative result of the bacterial culture and sensitivity of the fluid aspirate, the decision was made to discontinue antimicrobial therapy.

The filly was discharged from the hospital 3 weeks after surgery. Mild swelling of the ventral neck was still evident,

but the skin incision was dry, and the animal was otherwise in good general health with all vital and blood variables within normal limits. The owners were instructed to keep the filly on box rest for an additional 4 weeks. Hand walking was started approximately 2 months after surgery (10 minutes twice per day) and increased by 5 minutes per week for the following 6 weeks.

2.6 | Clinical outcome and follow-up

During clinical examination performed by the referring veterinary surgeon 8 weeks after surgery, the filly did not show any sign of lameness or ataxia, and results of the neurological examination were unremarkable. The cervical range of motion did not appear to be decreased, with no apparent restriction in dorsoventral or lateral head and neck movements. The surgical wound had healed completely, and there was no swelling in the area of the ventral neck.

The mare was turned out with other horses and continued to develop normally. Results of radiographic examination 9 months after surgery confirmed complete fusion of the atlantoaxial articulation with moderate callus formation present at the ventral aspect of the atlas and axis. All implants had remained in situ; there was a small radiolucent area evident at the cranial aspect of the plate (Figure 5). The mare showed free range of motion of the cervical



FIGURE 5 Left-lateral postoperative radiograph taken 9 months after surgical stabilization of a complete atlantoaxial luxation. Atlas and axis show physiological alignment, and all implants are in situ. There is moderate callus formation evident at the ventral aspect of the atlas and axis and a small radiolucency at the cranial aspect of the atlas

spine without obvious limitations and was scheduled to go into training 1 year after surgery.

3 | DISCUSSION

This report outlines the successful internal fixation of a complete luxation of the atlantoaxial articulation in an American Quarter Horse yearling. Luxations, subluxations, and fractures of the cranial cervical vertebrae may result from traumatic falls, collisions with solid objects, or halter accidents.^{6,10-20} In the described case, the yearling was reportedly kicked by another horse in the field. This trauma presumably led to severe hyperflexion of the cranial cervical spine with subsequent rupture of the ligaments attached to the dens, resulting in a complete luxation of the atlantoaxial articulation.

Spinal cord compression can occur with a complete luxation of the atlantoaxial articulation as the axis moves ventrally.⁶ The degree of neurological symptoms depends on the level of force acting on the spinal cord at the time of injury.⁶ In the described case, the yearling presented with no clinical signs of lameness or ataxia, and results of the neurological examination were unremarkable. However, advanced diagnostic imaging such as computed tomography or MRI would have allowed a more accurate evaluation of the associated soft tissue structures, including the spinal cord.²¹

To the best of the authors' knowledge, no successful surgical treatment has previously been reported for the complete luxation of the atlantoaxial articulation. For a subluxation of the atlantoaxial articulation with presence of neurological signs, the recommended surgical treatment has been an arthrodesis with a standard LCP or a distal femur LCP.^{6,7} For a complete luxation

of the atlantoaxial articulation, nonsurgical treatment is indicated, provided closed reduction is possible.^{6,22} The reduction of the luxation can be attempted by manipulation of the head and neck under general anesthesia; however, the successful reposition is usually possible only in acute injuries, and relaxation has been described.^{10,16,17,22} Manual reduction of the luxation was attempted within 48 hours after the trauma had occurred in the described case. To prevent iatrogenic trauma to the spinal cord, manual reduction was abandoned after several failed attempts. Because closed as well as open reduction of the complete luxation was unsuccessful, it was decided to remove the dens axis with an oscillating saw.¹² With this step, it was possible to achieve a physiological alignment of the atlas and axis and to apply an LCP to the ventral surface of both vertebrae (C₁ and C₂).

The 4.5-mm T-LCP that was used in the described case has recently been developed by DePuy Synthes in cooperation with the Large Animal Veterinary expert group of the AOVET foundation. Compared with the previous model, the new plate it is thicker and accepts either cortex or locking head screws. Compared with conventional plate and screw constructs, the angular and axial stability of locking head screws increases the strength of the construct under load without requiring precise anatomical contouring.²³ The three stacked combi holes that are arranged in the horizontal bar (T end) of the plate converge slightly (at a 95° angle), which allows the insertion of locking head screws with a length of up to 50 mm without interference of the screw tips. The described T-plate model has been successfully used for the internal fixation of tarsometatarsal subluxations, tarsometatarsal and distal intertarsal joint arthrodesis, and partial carpal arthrodesis.^{6,7,24} The application of this type of implant has also been described for the surgical treatment of physeal fractures of the proximal tibia in foals.²³ The biomechanical properties of the T-LCP are promising, and additional research including different areas of application in horses is warranted.^{6,24,25}

Seventy-three percent of the total axial rotation of the cervical spine occurs between the first and second cervical vertebrae.²⁶ To provide additional rotational and also dorsal stability, four 5.5-mm cortical screws were placed in lag fashion across the articular surface of the axis and the atlas. A similar technique without plate application has been described previously.¹⁰ On the basis of biomechanical assessment of pastern joint arthrodesis, the authors believe that the combination of transarticular screws and plate fixation have the advantage that joint instability is obviated by the plate while the transarticular screws provide compression across the entire joint space. The four oblique transarticular screws inserted in lag fashion counteract tensile forces at the dorsal aspect of the joint that might be induced by the plate. The additional stability gained by the combination of the transarticular screws and the ventral plate fixation reduce the

amount of cyclic loading acting upon each implant, which could result in screw loosening, especially in this location (A. Fürst, personal communication, 2018).

Seroma formation is a reported complication after cervical spinal surgery in horses.^{27,28} However, the authors chose not to use an active draining system to prevent ascending surgical site infection.

The described surgical approach resulted in the successful stabilization of a complete luxation of the atlantoaxial articulation with a favorable outcome in an American quarter horse yearling. A complete atlantoaxial luxation has historically been associated with a very poor prognosis for athletic function or even survival, especially in cases in which attempts of manual reduction were unsuccessful or caused damage to the spinal cord.^{8,16,29} This is the first report of surgical stabilization after a complete atlantoaxial luxation in a horse. While the horse did not show any neurological deficits or apparent reduction in cervical range of motion 9 months postoperatively, the development of osteoarthritis and potential impairment on future athletic performance cannot be excluded with certainty.

The described technique for atlantoaxial stabilization warrants validation in a larger cohort of horses. The use of the T-LCP may also have potential for application in similar pathologies, including fractures of the odontoid process or other types of destabilizing cervical vertebral fractures.

ACKNOWLEDGMENTS

The authors thank the support staff and students involved in the horses' care and the referring veterinary surgeon for sending the case.

CONFLICT OF INTEREST

None of the authors have any financial or personal relationships that could inappropriately influence or bias the content of this report.

REFERENCES

- Bainbridge D. The normal anatomy of the horse. In: Henson FMD, ed. *Equine Neck and Back Pathology*. 2nd ed. Hoboken, NJ: John Wiley & Sons; 2018:1-8.
- Nickel R, Schummer A, Seiferle E. *The Locomotor System of the Domestic Mammals*. 8th ed. Berlin, Germany: Verlag Paul Parley; 1986.
- Levine JM, Levine GJ, Hoffman AG, Mez J, Bretton GR. Comparative anatomy of the horse, ox, and dog: the vertebral column and peripheral nerves. *Compend Equine*. 2007;1:279-292.
- McCoy DJ, Shires PK, Beadle R. A ventral approach for stabilization of atlantoaxial subluxation secondary to an odontoid fracture in a foal. *J Am Vet Med Assoc*. 1984;185:545-549.
- Slone DE, Bergfeld WA, Walker TL. Surgical decompression for traumatic atlantoaxial subluxation in a weanling filly. *J Am Vet Med Assoc*. 1973;174:1234-1236.
- Funk KA, Erickson ED. A case of atlantoaxial subluxation in a horse. *Can Vet J*. 1968;9:120-123.
- Fürst AE. Vertebral column and spinal cord. In: Auer JA, Stick JA, eds. *Equine Surgery*. 5th ed. Philadelphia, PA: Saunders; 2018:864-894.
- Fürst A. AO Surgery Reference. Horse spine. <https://www2.aofoundation.org/wps/portal/surgery?showPage=approach&bone=HorseSpine&segment=Nonsegmented&Language=en>. Accessed June 28, 2019.
- Witte S, Alexander K, Bucellato M, et al. Congenital atlantoaxial luxation associated with malformation of the dens axis in a quarter horse foal. *Equine Vet Educ*. 2005;17:175-178.
- Ehrle A, Jones SJ, Klose P, Lischer C. Atypical radiologic appearance of a second vertebral fracture in a horse. *J Equine Vet Sci*. 2012;32:309-313.
- Nixon AJ. Fractures of the vertebrae. In: Nixon AJ, ed. *Equine Fracture Repair*. Philadelphia, PA: WB Saunders; 1996:299-312.
- Nixon AJ, Stashak TS. Laminectomy for relief of atlantoaxial subluxation in four horses. *J Am Vet Med Assoc*. 1988;193:677-682.
- Cillan-Garcia E, Taylor SE, Townsend N, Licka T. Partial osteotomy of the dens to correct atlantoaxial subluxation in a pony. *Vet Surg*. 2011;40:596-600.
- Nixon AJ. Surgical management of equine cervical vertebral malformation. *Prog Vet Neurol*. 1991;2:183-195.
- Robertson JT, Samii V. Traumatic disorders of the spinal column. In: Auer JA, Stick JA, eds. *Equine Surgery*. St Louis, MO: WB Saunders; 2006:677-683.
- Vaughan LC, Mason BJE. *A Clinico-Pathological Study of Racing Accidents in Horses: A Report of a Study on Equine Fatal Accidents on Racecourses Financed by the Horserace Betting Levy Board*. Vol 1973. Dorking, United Kingdom: Bartholomew Press:1-88.
- Licka T, Edinger H. Temporary successful closed reduction of an atlantoaxial luxation in a horse. *Vet Comp Orthop Traumatol*. 2002;13:146-148.
- Licka T. Closed reduction of an atlanto-occipital and atlantoaxial dislocation in a foal. *Vet Rec*. 2002;151:356-357.
- Rüedi M, Hagen R, Lüchinger U, Fürst A, Trump M. Subluxation von C2 und C3 und Fraktur von C2 nach einem schweren Schädelhirntrauma bei zwei Warmblutpferden. *Pferdeheilkunde*. 2011;27:522-527.
- Dyson SJ. The cervical spine and soft tissues. In: Ross MW, Dyson SJ, eds. *Diagnosis and Management of Lameness in the Horse*. St Louis, MO: Elsevier Science; 2003:522-531.
- Maier J, Zechmeister R, Schill W, Gerhards H, Liebich HG. Radiologic description of the growth plates of the atlas and axis in foals. *Tierarztl Prax Ausg G Grosstiere Nutztiere*. 1998;26(6):341-345.
- Gerlach K, Muggli L, Lempe A, Breuer J, Brehm W. Successful closed reduction of an atlantoaxial luxation in a mature warmblood horse. *Equine Vet Educ*. 2012;24:294-296.
- Lischer C, Rossignol F, Watkins JP. *AOTK System Innovations*. 2018. <https://view.joomag.com/aotk-system-innovations-2018-aotk-innovations-2018/0399541001544026356>. Accessed June 28, 2019.
- Keller SA, Fürst AE, Kircher P, et al. Locking compression plate fixation of equine tarsal subluxations. *Vet Surg*. 2015;44:949-957.

25. Curtiss AL, Goodrich LR, Rossignol F, Richardson DW. Pancarpal and partial carpal arthrodesis with 3 locking compression plates in 6 horses. *Vet Surg*. 2018;47:692-704.
26. Clayton HM, Townsend HGG. Kinematics of the cervical spine of the adult horse. *Equine Vet J*. 1989;21:189-192.
27. Kühnle C, Fürst A, Kümmerle J. Outcome of ventral fusion of two or three cervical vertebrae with a locking compression plate in 8 horses. *Vet Comp Orthop Traumatol*. 2018;3:356-363.
28. Rossignol F, Brandenberger O, Mespoules-Riviere C. Internal fixation of cervical fractures in three horses. *Vet Surg*. 2016;45:104-109.
29. Guffy MM, Coffman JR, Straffuss AC. Atlantoaxial luxation in a foal. *J Am Vet Med Assoc*. 1969;155:754-757.

How to cite this article: Schulze N, Ehrle A, Noguera Cender AC, Lischer C. Internal fixation of a complete ventral luxation of the dens axis in an American quarter horse yearling. *Veterinary Surgery*. 2019;48:1500–1506. <https://doi.org/10.1111/vsu.13283>

3.4 Arthroscopic removal of osteochondral fragments of the cervical articular process joints in three horses

Authors: Nicole Schulze; Anna Ehrle; Ina Beckmann; Christoph J. Lischer;

Publication: Equine Veterinary Surgery 2021;1–9.

DOI: 10.1111/vsu.13681

Correspondence Address:

Dr. med. vet. Nicole Schulze

Klinik für Pferde

Fachbereich Veterinärmedizin

Freie Universität Berlin, Oertzenweg 19B, 14163 Berlin

Phone: +49 30 838 622 99

Fax: +49 30 838 625 29

E-Mail: nicole.schulze@fu-berlin.de

Authorship: All authors were actively involved in the management of the cases and preparation of the manuscript.



SHORT CASE SERIES

WILEY

Arthroscopic removal of osteochondral fragments of the cervical articular process joints in three horses

Nicole Schulze | Anna Ehrle | Ina Beckmann | Christoph Lischer

Equine Clinic, Surgery and Radiology,
Freie Universität Berlin, Berlin, Germany

Correspondence

Nicole Schulze, Equine Clinic, Surgery
and Radiology, Freie Universität Berlin,
Oertzenweg 19 b, 14163 Berlin, Germany.
Email: nicole.schulze@fu-berlin.de

Abstract

Objective: To report arthroscopic osteochondral fragment removal from the equine cervical spine articular process joints (APJs) including long-term follow-up.

Study Design: Case series.

Animals: Three Warmblood horses with forelimb lameness and/or reduced range of motion of the cervical spine with osteochondral fragments between the cervical vertebrae C₅/C₆ or C₆/C₇.

Method: Arthroscopy of the APJs of C₅/C₆ and C₆/C₇ was performed under general anesthesia. Following endoscopic evaluation of the joints, osteochondral fragments were removed using a rongeur.

Results: All horses recovered from anesthesia with no anesthetic or minor postanesthetic complications. One horse needed a second procedure for fragment removal. Fourteen to 31 months post-surgery the horses were sound for their intended use and neurological examination revealed no abnormalities.

Conclusion: Arthroscopic removal of osteochondral fragments can be performed safely in the equine cervical APJs of C₅/C₆ and C₆/C₇ resulting in a favorable long-term outcome.

Clinical Significance: Arthroscopic removal is a valid option for horses showing clinical signs that can be attributed to osteochondral fragments in the APJs of the neck.

1 | INTRODUCTION

The equine cervical articular process joints (APJs) are bilateral intervertebral synovial diarthroses lined with hyaline cartilage.^{1–3} The APJs are located dorsal to the intervertebral foramina and extend medially towards the vertebral canal in the equine cervical spine.⁴ The flat, oval-shaped osseous components of the cervical APJs accommodate movement parallel to the articular surface.^{2–5} Caudal to the atlantoaxial articulation the joint surfaces are oriented obliquely, at approximately 45°–55°

to the horizontal plane, which increases further caudally as it progresses.⁶

Pathological conditions of the APJs include osteochondrosis dissecans (OCD), OCD-like lesions, fracture, and osteoarthritis.^{7–14} These disorders can limit athletic activity and lead to clinical signs like decreased cervical range of motion, forelimb lameness, weakness, proprioceptive deficits, and ataxia.^{9,15–19}

The etiology behind osteochondral fragments of cervical APJs is not yet fully understood. OCD and OCD-like lesions, as well as osteochondromatosis and fragmentation

This is an open access article under the terms of the Creative Commons Attribution License, which permits use, distribution and reproduction in any medium, provided the original work is properly cited.

© 2021 The Authors. *Veterinary Surgery* published by Wiley Periodicals LLC on behalf of American College of Veterinary Surgeons.

secondary to trauma are suggested as possible sources for these fragments.^{10,13,20,21}

The treatment of choice for the majority of osteochondral fragments located in other equine joints is arthroscopic removal.^{22,23} The arthroscopic approach and anatomy of the cervical APJs have been described recently.²⁴ Additionally, diagnostic arthroscopy of APJs (three horses) as well as a “cut down” arthroscopic approach for OCD fragment removal (one horse) have been described in clinical cases.^{10,24} In three out of the four reported cases, the horses were euthanized shortly after surgery due to deteriorating clinical signs or a poor prognosis for athletic activity.^{10,24} To the best of the author's knowledge, this is the first case series detailing successful arthroscopic osteochondral fragment removal in the equine cervical spine APJs including long-term follow-up.

2 | MATERIALS AND METHODS

2.1 | Case 1

2.1.1 | Clinical presentation

A 11-year-old Warmblood gelding (650 kg) was referred for further assessment of intermittent bilateral forelimb lameness of 2 years' duration, which was particularly noticeable during ridden exercise. The horse could no longer be used as a school horse. The lameness could not be localized to the forelimbs with diagnostic analgesia by the referring veterinarian and signs of neck stiffness had been observed.

Upon admission, the horse was bright, alert, and responsive. The physical examination including blood hematology and biochemistry was unremarkable. Lameness examination was performed with the support of a body-mounted inertial sensor system (lameness locator, Equinosis®). The horse did not show any sign of lameness at the walk and trot in a straight line on synthetic hard surface. Flexion tests were negative. During lunging (soft and hard surface) the horse kept the neck in a straight position and stumbled in the forelimbs. Under saddle an intermittent right forelimb lameness grade 1–2/5 (AAEP lameness score) was evident on the left rein. Symptoms were more noticeable on the right rein where the horse fell on its carpi when asked to trot on a small circle. The lateral range of motion of the cervical spine was moderately reduced to both sides. There was no heat, pain, or swelling on palpation in the area of the neck. No significant findings were revealed during a neurological examination, with the exception of stumbling while lunging with the neck flexed.

The horse was sedated (detomidine, 0.01 mg/kg intravenously [IV] and butorphanol, 0.05 mg/kg IV) and laterolateral, dorsoventral (C₁–C₂) and oblique (right 45°–55° ventral to left dorsal and left 45°–55° ventral to right dorsal) radiographs (Gierth HF400ML, Gierth X-Ray International GmbH, Riesa, Germany) of the cervical spine (C₁–T₁) were obtained.⁶ Radiographic examination identified an isolated round to oval radiopaque structure of approximately 1 cm diameter that was consistent with an osteochondral fragment at the cranial margin of the right C₅–C₆ cervical APJ (Figure 1A). Additionally, ultrasonography (Aplio 500, Canon Medical Systems GmbH, Neuss, Germany, 3 cm focus) of the APJs was performed. There was marked distention of the right C₅–C₆ APJ and the osteochondral fragment could be visualized at the cranial margin of the right C₅–C₆ cervical APJ.

2.1.2 | Surgical procedure

Flunixin meglumine (1.1 mg/kg IV), amoxicillin (10 mg/kg IV), and gentamicin sulfate (6.6 mg/kg IV) were administered preoperatively. For induction of general anesthesia the horse received medetomidine (7 µg/kg IV), diazepam (0.02 mg/kg IV), and ketamine (2.2 mg/kg IV).

The horse was placed under general anesthesia (isoflurane minimum alveolar concentration 1.0.) and xylazine (0.8 mg/kg/h IV) and positioned in left lateral recumbency. A 5-L fluid bag was positioned under the left C₅–C₆ cervical APJ in order to achieve slight left lateral flexion. A 42 × 43 cm digital radiography detector plate was placed between the operating table and the fluid bag centered on the C₅–C₆ articulation (Figure 2). Following aseptic preparation, the patient was draped routinely. Adhesive drapes were used at the surgical site to avoid the need for towel clamps that could interfere with the surgical procedure and intra-operative imaging. A 7.5-MHz straight linear array ultrasound transducer (Aplio 500, Canon Medical Systems GmbH, 3 cm focus) was covered with a sterile sleeve.

The location and orientation of arthroscopic portal to the right C₅–C₆ cervical APJ was identified with ultrasonography and radiography (Gierth HF400ML, Gierth X-Ray International GmbH) (Figure 3A) using lateral and oblique radiographic projections.^{6,25} Ultrasonography was considered necessary to improve orientation and reduce the risk of iatrogenic damage to the periarticular neurovascular structures.^{24–26} A point 1 cm cranial and 1 cm ventral to the C₅–C₆ APJ was determined radiographically. A 20G × 3½'' spinal needle was inserted under ultrasonographic guidance and directed in an approximately 60° cranioventral-caudodorsal angle to

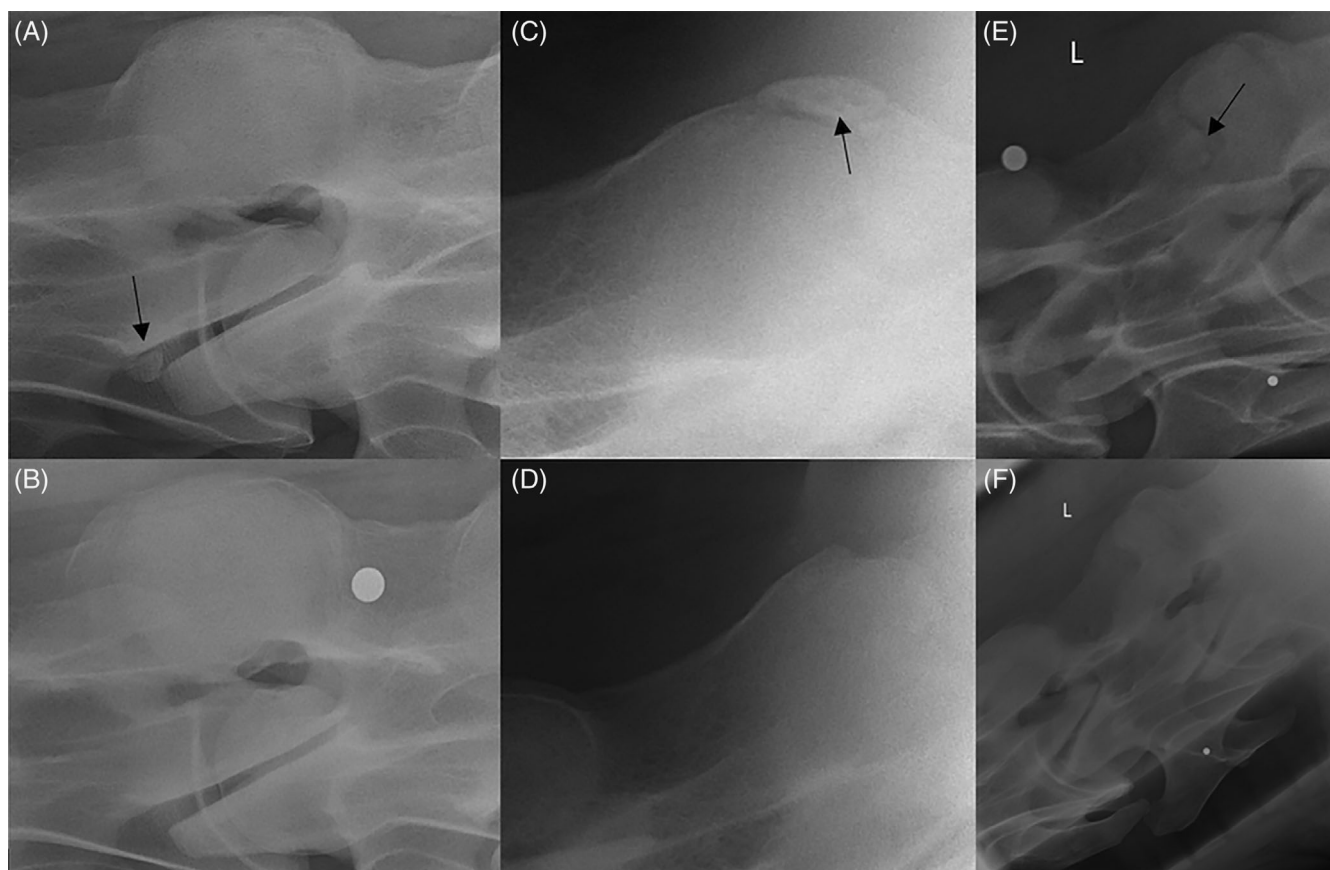


FIGURE 1 Case 1: (A) Left 45°–55° ventral to right dorsal preoperative radiograph showing isolated round to oval shaped radiopaque structure (black arrow) at the cranial aspect of the right C₅–C₆ cervical articular process joint (APJ). (B) Left 45°–55° ventral to right dorsal postoperative radiograph confirming successful removal of the OCD fragment. Case 2: (C) Left 45°–55° ventral to right dorsal preoperative radiograph highlighting isolated oval radiopaque structure (black arrow) consistent with an OCD fragment at the caudal aspect of the left C₆–C₇ cervical APJ. (D) Left 45°–55° ventral to right dorsal postoperative radiograph showing successful OCD fragment removal. Case 3: (E) Right 45°–55° ventral to left dorsal preoperative radiograph indicating OCD fragment (black arrow) at the cranial aspect of the right C₆–C₇ APJ. (F) Right 45°–55° ventral to left dorsal postoperative radiograph confirming successful fragment removal

reach the cranioventral joint recess at the visible joint space. The correct placement of the needle was confirmed radiographically and by aspiration of synovial fluid. Then, the joint was distended with 15 ml of sterile polyionic fluids. A 10-mm skin incision (No. 21 blade) was made at the point of the needle entry. The direction of the needle was subsequently followed with a No. 11 blade, creating a deep stab incision through the musculature overlying the APJ (*M. cutaneus colli* and *longissimus cervicis*).^{3,24} The arthroscopic cannula (4.0 mm, 30° forward-viewing arthroscope, length 18 cm, Karl Storz) and blunt obturator were guided into the cranioventral APJ compartment using ultrasonography and the position was confirmed radiographically with lateral and oblique projections before the obturator was replaced with the arthroscope (Figures 2 and 3A). A systematic evaluation of the cranioventral compartment including the cartilage, synovia, and subchondral bone of

the C₅–C₆ APJ was performed and the osteochondral fragment was located at the craniodorsal aspect of the right C₅ articular surface (Figure 4A). A second 20G × 3½" spinal needle was inserted into the cranioventral joint recess, approximately 2 cm craniodorsal to the arthroscope, to create an instrument portal using the technique described above. The osteochondral fragment was identified and elevated with a periosteal elevator (2 mm) and removed in one piece with a Ferris-Smith rongeur (4 mm, 14 cm straight). Debridement of the fragment bed was not required (Figure 4B). Multiple wear lines as well as superficial cartilage fibrillation were visible at the cranial and caudal surfaces of the C₅–C₆ articulation. The APJ was lavaged with approximately 1 L of sterile polyionic fluids before the skin was apposed in simple interrupted fashion (USP 2-0 polypropylene). The surgical site was protected with a stent bandage and assisted recovery was uneventful.

2.1.3 | Postoperative management and outcome

The gelding recovered from anesthesia with no anesthetic or postanesthetic complications with all vital parameters within normal limits. Mild to moderate wound swelling

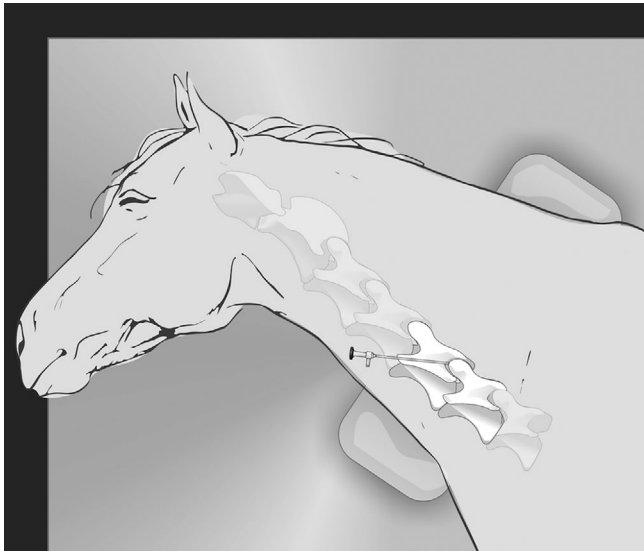


FIGURE 2 Graphic illustration of the anesthetized horse in lateral recumbency for the arthroscopic approach to the left C₅-C₆ articular process joint (APJ). A 5 L fluid bag or cushion is located under the C₅-C₆ APJ to achieve lateral joint flexion. Additionally, a digital radiography detector plate can be placed under the area of the C₅-C₆ articulation prior to surgery to facilitate intra-operative imaging. The arthroscope is positioned in the cranioventral joint compartment, inserted at a point 1 cm cranial and 1 cm ventral to the C₅-C₆ APJ and directed approximately 60° cranioventral-caudodorsal as performed for case 1 and case 3

was evident at the surgical site for 5 days. Hay and water were provided at shoulder height to avoid unnecessary neck movements. The stent was removed 4 days postoperatively. Antimicrobial therapy (amoxicillin 10 mg/kg IV every 8 h and gentamicin sulfate 6.6 mg/kg IV once daily) and Flunixin meglumine (1.1–0.5 mg/kg IV twice daily) were administered for 5 days (reducing to 0.5 mg/kg IV twice daily on day 4). Additionally, the horse received omeprazole (2 mg/kg orally once daily) during hospitalization. Repeated radiographs were obtained 1 day after surgery to confirm complete fragment removal (Figure 1B). The horse was discharged from the hospital 8 days after surgery when clinical examination revealed no abnormal findings. The owners were instructed to keep the gelding on box rest for a further 2 weeks. Hand walking commenced with 10 min twice a day and was increased by 5 min per week for the following 2 months.

Three months after surgery the gelding was re-examined at the referral hospital. The horse did not show any sign of lameness at the walk and trot in a straight line on synthetic hard surface. Flexion tests were negative. During lunging (soft and hard surface) the horse kept the neck still in a straight position, but the stumbling and the left forelimb lameness (1–2/5) were no longer visible. The lateral range of motion of the cervical spine was no longer reduced to both sides. A neurologic evaluation was within normal limits. Telephone follow-up 3 years after surgery confirmed that the gelding had remained in good general health and did not show any signs of lameness. The horse had returned to training 6 months post-surgery and was used as a riding school horse since.

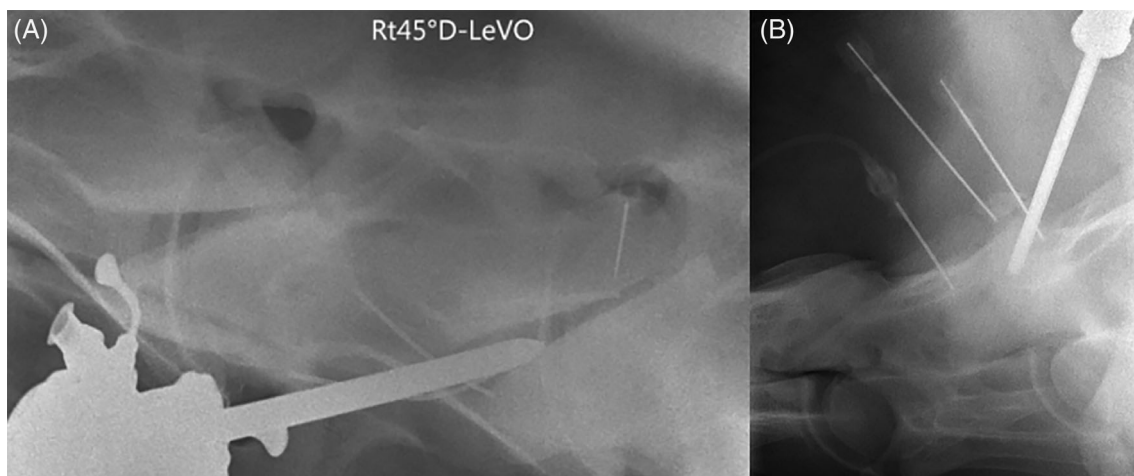


FIGURE 3 (A) Right 45°–55° dorsal to left ventral intra-operative radiograph of the C₅-C₆ articular process joint (APJ) with the arthroscopic cannula and blunt obturator in the cranioventral APJ compartment (case 1). Intra-operative radiography was used to confirm the correct position of the arthroscopic cannula before the obturator was replaced with the arthroscope. (B) Left 45°–55° ventral to right dorsal intra-operative radiograph of the C₆-C₇ APJ with the arthroscopic cannula in the caudodorsal APJ compartment (case 2)

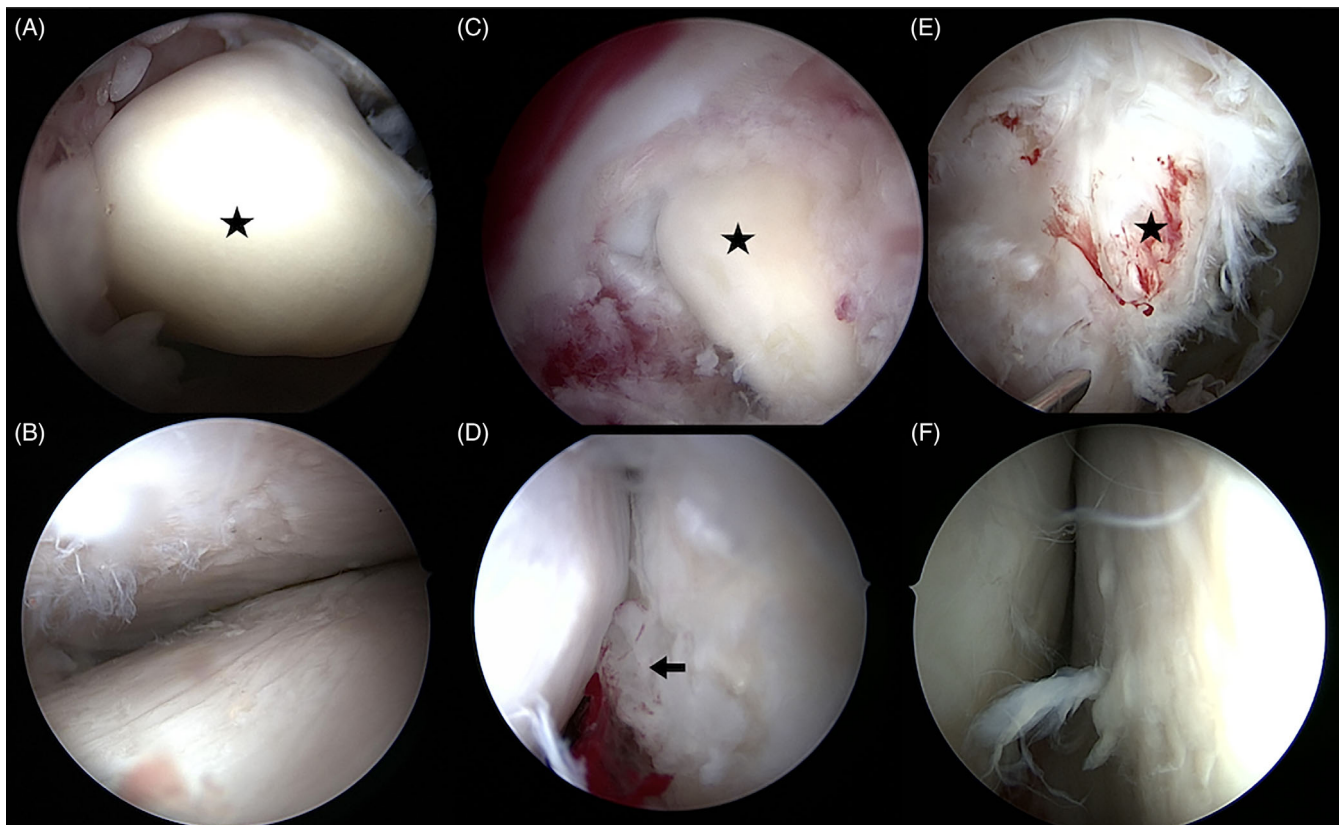


FIGURE 4 Case 1: (A) Arthroscopic view of the cranioventral recess of the right C₅-C₆ cervical articular process joint (APJ) showing a rounded osteochondral fragment (asterisk) associated with the craniodorsal aspect of the C₅ articular process. (B) Arthroscopic view of the cranioventral C₅-C₆ articular recess following fragment removal. Multiple wear lines as well as some mild cartilage fibrillations are evident at the right C₅-C₆ articular processes. Case 2: (C) Arthroscopic view of the caudodorsal recess of the left C₆-C₇ APJ. An osteochondral fragment (asterisk) is attached to the caudal aspect of the C₇ articular surface. (D) Arthroscopic view of the C₇ cranial articular surface after fragment removal. The fragment bed (arrowhead) was not debrided. Case 3: (E) Arthroscopic view of the cranioventral recess of the right C₆-C₇ cervical APJ. There is an oval shaped osteochondral fragment at the cranioventral aspect of the C₇ articular surface. (F) Arthroscopic view of the cranioventral C₆-C₇ articular recess following fragment removal showing multiple wear lines and superficial cartilage fibrillation at the surface of the C₆-C₇ articular processes. C₆ = right caudal articular process of C₆; C₇ = right cranial articular process of C₇

2.2 | Case 2

2.2.1 | Clinical presentation

A 6-year-old Warmblood showjumper gelding (660 kg) was referred for further assessment of left forelimb lameness of several weeks' duration that could not be eliminated with diagnostic analgesia. The referring veterinarian performed a complete perineural and intra-articular analgesia of the lame left forelimb up to the scapulohumeral joint.

The gelding presented bright, alert, and responsive. Physical examination was unremarkable with all vital parameters within normal limits. Dynamic examination identified grade 1-2/5 left forelimb lameness in a straight line on synthetic hard surface. The lameness was slightly more evident on the left rein (grade 2/5 left fore) when compared to the right rein (grade 1-2/5 left fore) on a soft and hard surface. A moderate reduction in cervical range of motion was noted on both

sides. There was no heat, pain, or swelling on palpation in the area of the neck or forelimbs. A full neurological examination was performed which was within normal limits.

Radiographic examination was performed based on the previously described protocol and confirmed the presence of an isolated round to oval shaped, radiopaque fragment at the caudodorsal aspect of the left C₆-C₇ cervical APJ (Figure 1C). Additionally, an ultrasonographic examination was performed based on the previously described protocol. There was marked distention of the left C₆-C₇ APJ and the osteochondral fragment could be visualized at the caudal margin of the left C₆-C₇ cervical APJ.

2.2.2 | Surgical procedure

The general setup including preoperative medication, induction and maintenance of general anesthesia,

positioning of the horse, aseptic preparation, draping, and intra-operative imaging were performed as detailed for case 1. The horse was however placed in right lateral recumbency as the left C₆-C₇ APJ was affected. The joint was distended (20 ml of sterile polyionic fluids) via needle insertion in the cranioventral recess under ultrasonographic guidance as described.²⁴ To access the caudodorsal recess of the C₆-C₇ APJ, a second 20G × 3½" spinal needle was inserted at a point approximately 4 cm caudal and 1 cm dorsal to the point where the first needle was placed. The needle was inserted in a 60° caudodorsal-cranioventral direction and fluid egress was noted from the needle hub. Subsequently, a stab incision for the arthroscopic portal was created using the needle as a guide for direction. However, placement of the arthroscopic cannula using the blunt obturator was not possible, despite ultrasonographic and radiographic guidance. After three unsuccessful attempts, the surgical procedure was aborted, and the horse was recovered from anesthesia without incident. A second attempt for arthroscopic fragment removal was made 4 weeks later. The clinical symptoms were unchanged from the initial examination. For the following surgery, the preoperative preparation and approach were as described as in the first case using the cranioventral approach. The creation of a caudodorsal approach was achieved by inserting a switching stick under arthroscopy guidance. Under arthroscopic guidance, the arthroscopic sleeve was inserted over the switching stick in the caudal compartment of the left C₆-C₇ APJ without difficulty (Figure 3B).

A systematic evaluation of the caudodorsal joint compartment was performed to localize the osteochondral fragment at the caudal aspect of the left C₇ articular surface (Figure 4C). A 20G × 3½" inch spinal needle was inserted into the caudodorsal APJ recess at a position approximately 2 cm cranial to the arthroscope, to indicate the direction for an instrument portal. A periosteal elevator was used to loosen the fragment that was subsequently removed with a Ferris-Smith rongeur in one piece. Debridement of the fragment bed was not required (Figure 4D). The joint was lavaged with polyionic fluids and skin closure and wound protection were performed as for case 1. Hand-assisted recovery was uneventful with no anesthetic or postanesthetic complications.

2.2.3 | Postoperative management and outcome

Successful fragment removal was confirmed radiographically (Figure 1D). The horse showed mild stiffness of the neck following surgery and additionally displayed subtle signs of colic with reduced appetite and fecal output after

the second surgery. All vital and blood parameters, trans-rectal palpation, and abdominal ultrasonographic examination were within normal limits and the horse responded rapidly to systemic analgesia (metamizole 40 mg/kg IV). Antimicrobial and anti-inflammatory medication including gastric protection was the same as in case 1. The horse was discharged from the hospital 2 weeks after surgery, with physical examinations remaining within normal limits. Rehabilitation instructions were as described above for case 1. Follow-up examinations were performed by the referring veterinarian 3, 7, and 17 months postoperatively.

The horse was in full training and performing according to expectations as a showjumper. Dynamic examination identified no lameness. The moderate reduction of the cervical range of motion was no longer evident on both sides.

2.3 | Case 3

2.3.1 | Clinical presentation

A 6-year-old Warmblood dressage horse gelding (550 kg) was admitted with a reduced range of motion of the neck that was particularly noticeable in flexion and when ridden on the right rein. A moderate reduction in lateral range of motion of the cervical spine to the right was evident.

The gelding was bright, alert, and responsive with all vital parameters within normal limits. Lameness and a complete neurological examination did not identify any significant findings. Radiographic (Figure 1E) as well as computed tomographic examination (Figure 5) showed an osteochondral fragment at the ventrolateral aspect of the right cranial articular surface of C₇. Computed tomography was performed by the referral clinic with the patient under general anesthesia with the neck in an extended position without myelography. The computed tomographic examination revealed a large defect in the subchondral bone of the right cranial articular process of C₇ that was in connection to the osteochondral fragment. A mild arthropathy of the right and left APJs between C₇/Th1 was diagnosed. No other findings in the cervical spine were detected.

2.3.2 | Surgical procedure

Surgery was performed as detailed for cases 1 and 2 with the horse placed in left lateral recumbency. A cranioventral approach was chosen due to the location of the fragment and aided by needle placement, joint

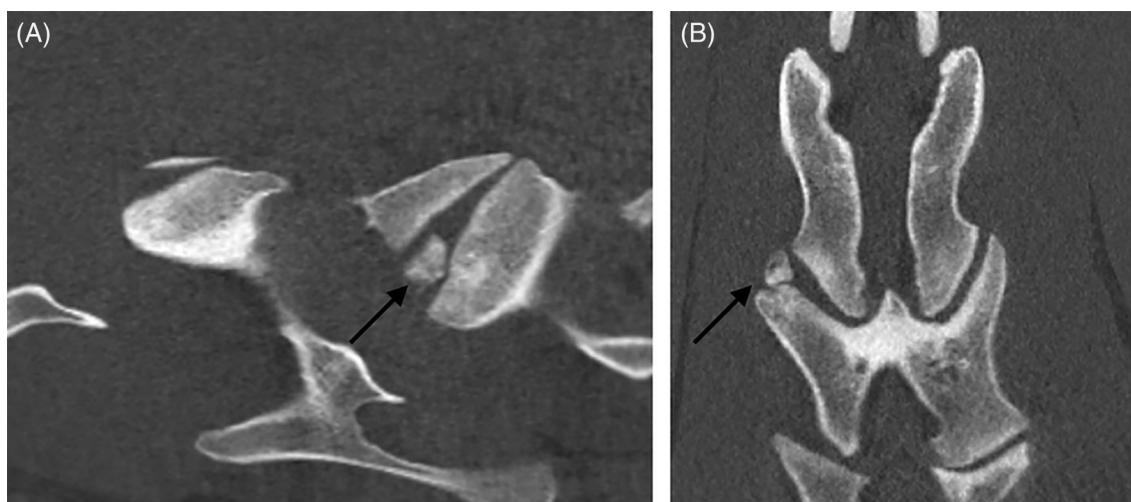


FIGURE 5 Sagittal (A) and frontal (dorsal) (B) computed tomographic images (32-detector-row CT scanner, Aquilion One, Canon Medical Systems) of the right C₆-C₇ articular process joint showing an osteochondral fragment (black arrow) associated with the cranio-lateral aspect of the right C₇ articular surface (case 3)

distention, and intra-operative imaging as described (Figure 2). The osteochondral fragment was localized at the ventrolateral aspect of the right cranial articular surface of C₇ (Figure 4E). An instrument portal was created cranial to the arthroscope and the fragment was elevated (periosteal elevator; 2 mm) and removed in one piece (Ferris-Smith rongeur; 14 cm straight; 4 mm). Moderate fibrillation and wear lines were noted in the hyaline cartilage of the cranial C₆-C₇ APJ (Figure 4F) and a large defect in the subchondral bone of C₇. Joint lavage, skin closure, wound protection, and recovery were performed as described for the above cases.

2.3.3 | Postoperative management and outcome

The gelding recovered from anesthesia with no anesthetic or postanesthetic complications and with all vital and blood parameters within normal limits. Antimicrobial therapy was discontinued. Flunixin meglumine (1.1–0.5 mg/kg IV twice daily) was administered for 5 days postoperatively (reducing to 0.5 mg/kg IV twice daily on day 4) and removal of the fragment was confirmed radiographically (Figure 1F). The horse was discharged from the hospital 12 days after surgery with examination parameters within normal limits. The owners were instructed to keep the gelding on box rest for further 3 weeks. Hand walking was started at 4 weeks (10 min twice a day) and increased by 5 min per week for the following 2 months.

Telephone follow-up 14 months after surgery with the referring veterinarian confirmed that the horse was

still in good general health and did not show any signs of lameness. The initial symptoms were no longer recognizable, and the horse was back in training and used as a dressage horse.

3 | DISCUSSION

This study outlines the arthroscopic evaluation of the caudal APJs (C₅/C₆ and C₆/C₇) with successful osteochondral fragment removal in three clinical cases.

The implications of osteochondral fragments in the equine cervical APJs are the subject of ongoing research.^{10,13,21} Clinical signs in pathological conditions of the APJs include decreased cervical range of motion, forelimb lameness, or ataxia.^{9,15–19}

The three cases outlined here all presented with a moderate reduction in cervical spine range of motion. In addition, cases 1 and 2 showed grade 1–2/5 forelimb lameness that did not respond to diagnostic analgesia and case 1 had additional neurological symptoms, noted as stumbling on the lunge line.

The clinical symptoms associated with the appearance of osteochondral fragments have not yet been clarified. Two recently published studies found osteochondral fragments in 22% and 24% of horses presented with cervical dysfunction.^{21,27} However, most of the cases also showed concurrent vertebral pathology. It would be all the more important to clarify the clinical significance by means of diagnostic anesthesia, but so far there is little information on this. Recently an ultrasonographic-guided injection of the medial branch of the dorsal ramus of the cervical spinal nerves in cadaveric equine necks was

developed.²⁶ However, clinical studies in this field are still lacking.^{17,18} Until then, it will remain difficult to definitively identify the clinical significance of these osteochondral fragments. In the three cases presented here, the initial symptoms improved postoperatively and all horses were sound for their intended use. None of the horses received additional treatments postoperatively.

CT examination was performed to further assess the osteochondral fragment including its exact location and concurrent cervical spinal pathology in case 3 by the referral clinic. Apart from a mild arthropathy of the APJs between C₇/Th₁, there were no other findings that could have questioned the clinical significance of the symptoms in this case. Nevertheless, it is not uncommon in horses with APJs Osteochondral fragmentation to find additional cervical pathology, which can complicate the interpretation of clinical significance.²¹

The increasing availability of large gantry CT apertures in equine referral practice as well as detailed reports on the use of CT and CT myelography for the detection of cervical spinal lesions facilitate a comprehensive evaluation of APJ osteochondral fragments and associated pathology in equine patients.^{21,27} A myelogram to rule out stenosis may additionally be indicated in some cases.

The horses were positioned with the affected APJ in lateral flexion to achieve slight opening of the joint space and optimize arthroscopic access to the cranioventral joint.^{5,10,24} Mechanical distraction of the APJ to avoid collapse of the joint capsule caused by fluid extravasation as described for other joints was not performed.²⁴ It is however likely that extravasation has complicated the approach to the caudodorsal C₆-C₇ APJ during the initial surgical attempt in case 2. In line with the first report detailing the technique, the arthroscopy of the most caudal APJs (C₆-C₇) was also considered more difficult when compared to the C₅-C₆ articulation.²⁴ The overlying musculature of the shoulder region impaired on the movability of the arthroscopic sleeve, particularly during the approach to the caudodorsal C₆-C₇ APJ recess (case 2), where it is required to manipulate the arthroscope at 60°–80° to the long axis of the neck in a caudodorsal-cranioventral direction. Based on this experience we would recommend to use the cranioventral approach to place the first arthroscopic portal irrespective of the location of the osteochondral fragment.

One limitation for this case series is that the lameness examinations did not include the use of local anesthesia to further localize the lesion to the affected APJ. The inconsistent nature of the lameness in two of the horses as well as lack of lameness in the third would have made the evaluation the effects of diagnostic analgesia in these horses difficult. The addition of a CT examination as well

as myelography may have also improved localization of the neck abnormalities to the APJ in the first two cases; however, it was not available for use at the time of the exam. Finally, histologic evaluation of the fragments removed may have been useful to establish a diagnosis and should be recommended in future cases to provide evidence for a possible etiology of APJ fragments.

In conclusion, arthroscopic removal of osteochondral fragments in the equine cervical APJs can be performed safely, with a good prognosis for return to athletic function in horses with low-grade lameness and mild neurologic deficits. In the horses in this report, no negative effects were associated with the surgical procedure, and the clinical signs noted prior to surgery were improved allowing return to their intended use. Arthroscopic removal of APJ fragments may be considered as an approach to treat these lesions, but a clear link between clinical signs and the fragments has not yet been proven. Therefore, operating a larger number of horses will also help establish the clinical significance of these fragments.

ACKNOWLEDGMENTS

The authors would like to acknowledge the support staff and students involved in the horses' care and the referring veterinary surgeons for sending the cases. Open Access funding enabled and organized by Projekt DEAL.

CONFLICT OF INTEREST

None of the authors has any financial or personal relationships that could inappropriately influence or bias the content of the paper.

AUTHOR CONTRIBUTIONS

All authors were actively involved in the management of the cases and preparation of the manuscript.

REFERENCES

1. Henson FMD. *Equine Neck and Back Pathology*. 2nd ed. Oxford: John Wiley & Sons Ltd; 2018.
2. O'Leary SA, White JL, Hu JC, Athanasiou KA. Biochemical and biomechanical characterization of equine cervical facet joint cartilage. *Equine Vet J*. 2018;50:800-808.
3. Nickel R, Schummer A, Seiferle E. *The Locomotor System of the Domestic Mammals*. Berlin: Verlag Paul Parley; 1986.
4. Claridge HAH, Piercy RJ, Parry A, Weller R. The 3D anatomy of the cervical articular process joints in the horse and their topographical relationship to the spinal cord. *Equine Vet J*. 2010;42:726-731.
5. Clayton HM, Townsend HG. Kinematics of the cervical spine of the adult horse. *Equine Vet J*. 1989a;21:189-192.
6. Whithers JM, Voute LC, Hammond G, Lischer CJ. Radiographic anatomy of the articular process joints of the caudal cervical vertebrae in the horse on lateral and oblique projections. *Equine Vet J*. 2009;41:895-902.

7. Pool RR. Difficulties in definition of equine osteochondrosis; differentiation of developmental and acquired lesions. *Equine Vet J Suppl.* 1993;16:5-12.
8. Rooney JR. Osteochondrosis in the horse. *Mod Vet Pract.* 1975; 56:41-43.
9. Powers BE, Stashak TS, Nixon AJ, Yovich JV, Nordin RW. Pathology of the vertebral column of horses with cervical static stenosis. *Vet Pathol.* 1988;23:392-399.
10. Tucker R, Piercy RJ, Dixon JJ, et al. Arthroscopic treatment of cervical articular process joint osteochondrosis in a thoroughbred horse. *Equine Vet Educ.* 2018;30:116-121.
11. Beck C, Middleton D, Maclean A, Lavelle R. Osteochondrosis of the second cervical vertebra of a horse. *Equine Vet J.* 2002; 34:210-212.
12. Bergmann W, de Mik-van Mourik M, Veraa S, et al. Cervical articular process joint osteochondrosis in Warmblood foals. *Equine Vet J.* 2020;52(5):664-669.
13. Lim CK, Hawkins JF, Vanderpool AL, Heng HG, Gillespie Harmon CC, Lenz SD. Osteochondritis dissecans-like lesions of the occipital condyle and cervical articular process joints in a Saddlebred colt horse. *Acta Vet Scand.* 2017;59 (1):76.
14. Janes JG, Garrett KS, McQuerry KJ, et al. Cervical vertebral lesions in equine stenotic myelopathy. *Vet Pathol.* 2015;52(5): 919-927.
15. Trostle S, Dubielzig R, Beck K. Examination of frozen cross sections of cervical spinal intersegments in nine horses with cervical vertebral malformation: lesions associated with spinal cord compression. *J Vet Diagn Invest.* 1993;5: 423-431.
16. Stewart RH, Reed SM, Weisbrode SE. Frequency and severity of osteochondrosis in horses with cervical stenotic myelopathy. *Am J Vet Res.* 1991;52:873.
17. Ricardi G, Dyson SJ. Forelimb lameness associated with radiographic abnormalities of the cervical vertebrae. *Equine Vet J.* 1993;25(5):422-426.
18. Dyson SJ. Lesions of the equine neck resulting in lameness or poor performance. *Vet Clin North Am Equine Pract.* 2011;27(3): 417-437.
19. García-López JM. Neck, back, and pelvic pain in sport horses. *Vet Clin North Am Equine Pract.* 2018;34(2):235-251.
20. Moore BR, Holbrook TC, Stefanacci JD, Reed SM, Tate LP, Menard MC. Contrast-enhanced computed tomography and myelography in six horses with cervical stenotic myelopathy. *Equine Vet J.* 1992;24:197-202.
21. Tucker R, Hall YS, Hughes TK, Parker RA. Osteochondral fragmentation of the cervical articular process joints. *Equine Vet J.* 2021;00:1-8. <https://doi.org/10.1111/EVJ.13410>
22. McIlwraith CW. Surgical versus conservative management of osteochondrosis. *Vet J.* 2013;197:19-28.
23. McIlwraith CW, Foerner JJ, Davis DM. Osteochondritis dissecans of the tarsocrural joint: results of treatment with arthroscopic surgery. *Equine Vet J.* 1991;23:155-162.
24. Pepe M, Angelone M, Gialletti R, Nannarone S, Beccati F. Arthroscopic anatomy of the equine cervical articular process joints. *Equine Vet J.* 2014;46:345-351.
25. Berg LC, Nielsen JV, Thoenner MB, Thomsen PD. Ultrasonography of the equine cervical region: a descriptive study in eight horses. *Equine Vet J.* 2003;35:647-655.
26. Corraletti G, Vandeweerd JM, Hontoir F, Vanderperren K, Palmers K. Anatomy and ultrasound-guided injection of the medial branch of the dorsal ramus of the cervical spinal nerves in the horse: a cadaveric study. *Vet Comp Orthop Traumatol.* 2020;33:377-386. <https://doi.org/10.1055/s-0050-1714301>
27. Gough SL, Anderson JDC, Dixon JJ. Computed tomographic cervical myelography in horses: technique and findings in 51 clinical cases. *J Vet Intern Med.* 2020;33:377-386. <https://doi.org/10.1111/jvim.15848>

How to cite this article: Schulze N, Ehrle A, Beckmann I, Lischer C. Arthroscopic removal of osteochondral fragments of the cervical articular process joints in three horses. *Veterinary Surgery.* 2021;1-9. <https://doi.org/10.1111/vsu.13681>

4 Discussion

New insights into the dynamics of the joint components of the APJ during motion could be gained using dynamic 2D and 3D CT. Furthermore, specific motion segments could be evaluated in all motion directions (axial rotation, dorso-ventral flexion and lateral bending). As a specific result, no significant increase in range of motion was found after fusion of the C3/4 motion segment in the adjacent segments (C2/3 and C4/5) in equine cadaver necks.

Static computed tomography is an advanced diagnostic imaging technique that is of great importance in the evaluation of fracture configurations in horses and is frequently used in preoperative planning, among other applications (Gasiorowski et al. 2015; Puchlaski et al. 2007; Jackson et al. 2019).

Wide area-detector CT scanners are particularly useful for dynamic studies because they provide high temporal resolution and whole-joint coverage during sequential acquisition (Gondim et al. 2015). This offers the possibility to show the interaction of joint components during complex movements as multiple image volumes are recorded over time and subsequently reviewed in form of a video sequence (Gondim et al. 2015; White et al. 2019). Dynamic CT has been introduced in human orthopedics over the past decade and is gaining increasing popularity, but to the authors' knowledge the technique is not yet used in the veterinary field (Gondim et al. 2017; De Preux et al. 2020).

While in human medicine the patient is fully conscious and actively performs controlled movements during the dynamic CT scan, sedation or general anesthesia would be mandatory in veterinary patients to image controlled movement patterns. Other challenges to the widespread use of dynamic CT in routine diagnostic imaging include the cost of the scanner and the handling and processing of the large volumetric data sets generated by this technique (Kwong et al. 2015). In the study described, constant and continuous motion of the C4/5 spinal motion segment was achieved using a motor-driven external device (Schulze et al. 2020). Although the application of dynamic CT in horses is more technically challenging compared with human or small animal patients, the development of similar devices may be useful for the examination of other body regions, including the distal limbs of the horse.

Overall, image quality was excellent for both flexion and extension motion focused on the C4/5 motion segment of 2D and 3D video sequences derived from CT data in the sagittal plane. There were some minor motion artifacts present in the 2D-CT videos in both flexion and extension. These can be explained by the higher velocity of movement of the soft tissues compared to the APJs. Whilst motion artifacts can impair on image analysis and post-

processing, it has been demonstrated that the assessment of axial CT sequences is not qualitatively affected by object motion at 0.05m/sec (Gondim et al. 2017). Since each individual dynamic CT scan consists of several individual sequences, it was ensured that at least one sequence was free of motion facts and diagnostically evaluable.

The volume acquisition speed depends on the rotation speed of the gantry and the image reconstruction technique and is the most important parameter for controlling motion artifacts (Beeres et al. 2015; Grosjean et al. 2007). The highest gantry rotation speed was used for the dynamic CT examinations (0.05 m/sec), as it has already been shown in previous studies that lower acquisition speeds lead to an exponential decrease in image quality (Dawson and Lees 2001; Schulze et al. 2020).

As shown in previous studies, there was an increase in range of motion in the caudal motion segments of the cervical spine during flexion-extension and lateral bending in the current study (Clayton and Townsend 1989a). This was significantly greater than in the cranial motion segments of the cervical spine. One possible explanation for the larger range of motion in the caudal cervical spine is thought to be the more medial orientation of the articular process joints in this region, facilitating an increased range of motion (Clayton and Townsend 1989a; Zsoldos et al. 2010).

ASD is thought to be caused by an increase in range of motion and higher loads acting upon adjacent motion segments after intervertebral fusion (Ahmed et al. 2017). The pathogenesis is largely unknown, and the study of the condition relies mainly on in vitro studies, yet disc degeneration is the most common pathologic feature observed (Volkheimer et al. 2015; Matsunaga et al. 1999).

In multiple studies in canine and humans using all different devices used for intervertebral fusion, including the locking compression plate construct used in the current study, there was a significant increase in the range of motion of the adjacent segment (Hakozaki et al. 2016; Schwab et al. 2006).

However, in contrast to the canine and human studies, the range of motion of the adjacent segments did not change significantly after fusion in the equine cervical spine specimens. In human medicine the debate is ongoing as to whether adjacent segment disease develops due to the increased biomechanical load on the intervertebral discs adjacent to the cervical fusion sites or is caused by pre-existing degenerative disc disease, characterized by disc fragmentation or protrusion (Ahmed et al. 2017).

To the authors' knowledge, there are no scientific studies on the significance of disc degeneration in horses. Only a small number of case reports suggest that neurologic deficits may be associated with equine disc lesions (Foss et al. 1983; Furr et al. 1991; Fuentealba Et al 1991). As the intervertebral pressure in the area of the intervertebral discs was not assessed in the current study further investigation of the clinical significance of intervertebral disc degeneration as well as intervertebral pressure measurements of adjacent segments before and after intervertebral fusion is required.

In addition, the dynamic CT data were used to further investigate the detailed movement pattern of equine cervical APJs.

In general, it was found that the translational displacement of the articular surfaces of the cervical spine is significantly greater in flexion than in extension. Relative to the mean length of the APJ surface, the mean displacement of the APJ surface in flexion was over 43% and in extension only about 7%.

At full flexion, the 2D videos showed that the cranial margin of C5 was in close proximity to the C4 articular surface. At full extension, the caudal margin of C5 was in close proximity to the C4 articular surface. Thus, impingement can easily occur in the area of these contact points. The increased pressure at these contact points could potentially contribute to the development of osteochondrosis or osteoarthritis in this area. The exact etiopathogenesis of cervical APJ osteoarthritis and osteochondrosis is not yet clear (DeRouen et al. 2016; Birmingham et al. 2010; Pepe et al. 2014).

The limitations of the first two publications include the ex-vivo protocol of the study, and the small number of specimens. The spines were excised at the level of the atlanto-occipital and cervicothoracic junction, leaving only the perivertebral muscles and joint capsules intact. This has been described previously in other studies (Sleutjens et al. 2014; Clayton et al. 1989a). Because of the excision, spinal mobility may have been affected compared with ROM of the entire equine cervical spine. The fixation of the cervical spine specimen could have impaired on the motion segments range of motion. However, the two motion segments cranial and caudal to the fused segment were not attached to the testing device during CT evaluation. The forces acting upon the equine cervical spine during physiological movement are described to lie at approximately 40 to 80 Joules (Gellman und Bertram 2002). When a force of 50 Nm was applied in the current study this equated 25 to 50 times the force applied in the canine study and no further movement could be elicited by application of a force greater than 50 Nm (1 Joules $\frac{1}{4}$ 1 Nm) (Hakozaki et al. 2016).

The postmortem evaluation of the specimens does not take the entire function of the ligaments and musculature into account and only gives a momentary state rather than an

assessment over time. While osteoarthritis and secondary changes can strongly influence the kinetics of the cervical spine, no pre-existing pathological conditions were noted in the specimens used for the study.

As shown in these *ex vivo* studies, the resulting pressure in full extension or flexion at the contact points on the articular surface of C4/5 could potentially contribute to the development of osteochondrosis or osteoarthritis. The implications of osteochondral fragments in the equine cervical APJs are the subject of ongoing research (Tucker et al 2018; O'Leary et al 2018; Thomsen et al. 2013).

Clinical signs in pathological conditions of the APJs are nonspecific and like other symptoms in cervical spine disorders including decreased cervical range of motion, forelimb lameness, or ataxia (Tucker et al. 2021; Thomsen et al 2013; Pérez-Nogués et al. 2020; García-López 2018; Dyson 2020). The three horses described in the case report all had limited range of motion of the cervical spine and in some cases mild forelimb lameness that did not respond to diagnostic analgesia. One case had additional neurological symptoms. In these three cases we were able to evaluate the caudal APJs (C5/C6 and C6/7) and to remove osteochondral fragments in the APJs arthroscopically.

The clinical symptoms associated with the appearance of osteochondral fragments of the APJs have not yet been clarified. Two recently published studies found osteochondral fragments in 22% and 24% of horses presented with cervical dysfunction (Tucker et al. 2021; Gough et al. 2020). However, most of the cases also showed concurrent vertebral pathology. It would therefore be of particular interest to clarify the clinical significance of these fragments using diagnostic anesthesia. However, clinical studies in this field are still lacking. In the three cases presented here, the initial symptoms improved after arthroscopic removal and all horses were sound for their intended use thereafter. None of the horses received additional treatments postoperatively.

For surgery the horses were positioned with the affected APJ in lateral flexion to achieve slight opening of the joint space and optimize arthroscopic access to the cranioventral joint (Tucker et al. 2018; Pepe et al. 2014). Consistent with the first report describing the technique, arthroscopy of the most caudal APJs (C6-C7) was also found to be more difficult compared with C5-C6 articulation (Pepe et al. 2014). Particularly when accessing the caudodorsal C6-C7 APJ recess, the overlying musculature of the shoulder region impairs the mobility of the arthroscopic sleeve. Based on this experience, we recommend creating the

first arthroscopic portal via the cranioventral approach, regardless of the location of the osteochondral fragment.

A limitation of this case series is that local anesthesia was not performed to further localize the lesion in the affected APJ. The inconsistent nature of the lameness in two of the horses as well as lack of lameness in the third would have made the evaluation the effects of diagnostic analgesia in these horses difficult. The addition of a CT examination as well as myelography may have also improved localization of the neck abnormalities to the APJ in the first two cases; however, it was not available for use at the time of the exam. Finally, histologic evaluation of the fragments removed may have been useful to establish a diagnosis and should be recommended in future cases to provide evidence for a possible etiology of APJ fragments and their association with the clinical signs.

The second case report describes the first successfully internal fixation of a complete luxation of the atlantoaxial articulation in a horse. The American Quarter Horse yearling was reportedly kicked by another horse while in the pasture. Usually, subluxation / luxation result from traumatic falls, collisions with solid objects, or halter accidents (Funk and Erickson 1968; Dyson 2003; Rüedi et al. 2011; Licka 2002; Licka and Edinger 2002; Auer and Stick 2018; Nixon 1991; Nixon 1996; Nixon and Stashak 1988; Ehrle et al. 2012). Presumably, this kick resulted in severe hyperflexion of the cranial cervical spine with subsequent rupture of the ligaments attached to the dens, leading to complete luxation of the atlantoaxial joint. Complete luxation or subluxation of the atlantoaxial joint can result in spinal cord compression as the axis moves ventrally (Funk and Erickson 1968).

No successful surgical treatment has previously been reported for the complete luxation of the atlantoaxial articulation. The recommended surgical treatment for a subluxation of the atlantoaxial articulation with presence of neurological signs is cervical ventral fusion (arthrodesis) with a standard LCP or a distal femur LCP (Funk and Erickson 1968; Auer and Stick 2018).

For a complete luxation of the atlantoaxial articulation, nonsurgical treatment is indicated, provided closed reduction is possible (Funk and Erickson 1968; Gerlach et al. 2012). Reduction of the luxation can be attempted by manipulation of the head and neck under general anesthesia; however, the successful reposition is usually possible only in acute injuries, and reluxation has been described (Gerlach et al. 2012; Ehrle et al. 2012; Licka and Edinger 2012).

In this case manual reduction of the luxation was attempted within 48 hours after the trauma had occurred in the described case. After several failed attempts manual reduction was abandoned to prevent iatrogenic trauma to the spinal cord. Open reduction of the complete dislocation was also unsuccessful. Therefore, it was decided to remove the dens axis with an oscillating saw to achieve physiological alignment of the atlas and axis, and to apply an LCP to the ventral surface of both vertebrae (C1 and C2).

In contrast to the cervical vertebral fusion of the C3/4 motion where a 4.5 mm LCP was used, in this case a 4.5 mm T-LCP, was used. This was recently developed by DePuy Synthes in collaboration with the Large Animal Expert Group of the AOVET Foundation.

Compared to the normal plate and screw constructs, the angular and axial stability of locking head screws increases the strength of the construct under load without the need for precise anatomical contouring (Lischer et al. 2019). Compared to the previous model, the new plate is thicker and accepts either cortical or locking screws. The special feature of the plate includes the three stacked combi-holes arranged in the horizontal bar (T-end) of the plate. They converge slightly (at an angle of 95), which allows the insertion of locking head screws with a length of up to 50 mm without interference of the screw tips. The T-plate has already been successfully used for a wide variety of indications. For example, for the internal fixation of tarsometatarsal subluxations, tarsometatarsal and distal intertarsal joint arthrodesis, and partial carpal arthrodesis (Funk and Erickson 1968; Auer and Stick 2018; Keller et al. 2015). The use of the implant has also been described for the surgical treatment of physeal fractures of the proximal tibia in foals (Lischer et al. 2019).

The authors believe that the combination of transarticular screws and plate fixation have the advantage that joint instability is obviated by the plate while the transarticular screws provide compression across the entire joint space. The four oblique transarticular screws inserted in lag fashion counteract tensile forces at the dorsal aspect of the joint that might be induced by the plate. The additional stability gained by the combination of the transarticular screws and the ventral plate fixation reduce the amount of cyclic loading acting upon each implant, which could result in screw loosening, especially in this location (A. Fürst, personal communication, 2018).

The results of radiographic examination 9 months after surgery confirmed complete fusion of the atlantoaxial joint with moderate callus formation on the ventral aspect of the atlas and axis. All implants had remained in place. The mare showed free range of motion of the cervical spine with no obvious limitations and entered training 1 year after surgery.

5 Zusammenfassung

Neue chirurgische Techniken der Halswirbelsäulen Chirurgie bei Pferden

Eine neue CT-Generation mit einer Detektorabdeckung von 16 cm und einer Rotationsgeschwindigkeit von 0,32 Sekunden/Umdrehung ermöglicht es, qualitativ hochwertige dreidimensionale Bilder des zervikalen Gelenkfortsatzes C4/5 des Pferdes in Bewegung zu generieren. Die dynamische CT-Bildgebung erlaubt neue Einblicke in die Bewegungsmuster von Gelenkbewegungssegmenten, was für die Untersuchung von Facettengelenken und anderen Gelenkerkrankungen von Nutzen sein kann. Die Studie ist ein erster Schritt zur Untersuchung des Potenzials der dynamischen 3D-CT in der Veterinärmedizin, einer Technik, die erst seit kurzem erforscht wird und vor ihrer Einführung in die Routinepraxis noch viel Raum für Verbesserungen lässt.

Außerdem zeigte die ex-vivo Studie keinen signifikanten Zusammenhang zwischen der Fusion eines zervikalen Bewegungssegments und der Veränderung des Bewegungsumfangs der angrenzenden Wirbelsegmente. Abgesehen von einer Erkrankung des angrenzenden Segments aufgrund einer Vergrößerung des Bewegungsumfangs der angrenzenden Wirbelsegmente wird jedoch bei anderen Spezies nach einer Wirbelversteifung häufig eine benachbarte degenerative Bandscheibenerkrankung diagnostiziert. Der erhöhte Druck, der nach einer Fusion der benachbarten Wirbelsegmente auf das Zwischenwirbelgelenk einwirkt, kann sich auch auf die Bandscheibe bei Pferden auswirken. Weitere Untersuchungen zu den Auswirkungen der Wirbelfusion auf den Bandscheibendruck in der Halswirbelsäule von Pferden sind angezeigt.

Zum ersten Mal wurde eine erfolgreiche chirurgische Technik zur Stabilisierung einer vollständigen Luxation des atlantoaxialen Gelenkes bei einem amerikanischen Quarter Horse Jährling beschrieben. Eine vollständige atlantoaxiale Luxation war in der Vergangenheit mit einer sehr schlechten Prognose für die sportliche Funktion oder sogar das Überleben verbunden, insbesondere in Fällen, in denen manuelle Repositionsversuche erfolglos waren oder das Rückenmark geschädigt hatten (Fürst 2019; Vaughan et al. 1973; Guffy et al. 1969). Neun Monate nach der Operation, waren die Halswirbel C1 und C2 knöchern überbrückt und das Pferd zeigte weder neurologischen Defizite noch offensichtliche Einschränkung des zervikalen Bewegungsumfangs. Weitere Fälle sind nötig, um die Methode zu bewerten und die Langzeitprognose zu evaluieren.

In einer kleinen Fallserie konnten wir zeigen, dass die arthroskopische Entfernung von osteochondralen Fragmenten in den zervikalen APJs von Pferden sicher durchgeführt werden kann. Bei Pferden mit geringgradiger Lahmheit und leichten neurologischen Symptomen kann die arthroskopische Entfernung von APJ-Fragmenten mit guter Prognose als Behandlungsmethode in Betracht gezogen werden. Ein eindeutiger Zusammenhang zwischen den klinischen Symptomen und den Fragmenten konnte jedoch noch nicht sicher nachgewiesen werden. Hierfür ist die chirurgische Behandlung einer größeren Anzahl von Pferden nötig.

6 Summary

A new CT generation with a detector coverage of 16 cm and a rotation speed of 0.32 seconds / rotation makes it possible to obtain high quality images of equine cervical articular process joint C4/5 in motion. This work further confirms that dynamic CT imaging has the potential to provide new insight into the movement pattern of articular motion segments, which may be of value for the examination of APJ and other joint conditions. The study provides a first step in the investigation of the potential of dynamic 3D CT in veterinary medicine, a technique that has only begun to be explored and leaves much room for refinement prior to its introduction in routine practice.

Additionally, the ex-vivo study did not show any significant association between fusion of a cervical motion segment and change in range of motion of the adjacent vertebral segments. However, apart from adjacent segment disease due to an increase in range of motion of adjacent vertebral segments, adjacent degenerative disc disease is commonly diagnosed in other species after vertebral fusion. Increased pressure acting on the intervertebral joint after adjacent vertebral fusion may also affect the intervertebral disc in the equine patient. Further research investigating the implications of vertebral fusion on the intervertebral pressure in the equine cervical spine is indicated.

For the first time, a surgical approach to stabilize complete luxation of the atlantoaxial articulation in an American quarter horse yearling has been successfully performed. A complete atlantoaxial luxation has historically been associated with a very poor prognosis for athletic function or even survival, especially in cases in which attempts of manual reduction were unsuccessful or caused damage to the spinal cord (Fürst 2019; Vaughan et al. 1973; Guffy et al. 1969). Nine months postoperatively, bony fusion between C1 and C2 was radiographically evident, the horse did not show any neurological deficits or apparent reduction in cervical range of motion. More cases are required to evaluate the surgical technique and the long-term outcome.

A small case series revealed that arthroscopic removal of osteochondral fragments in the equine cervical APJs can be performed safely, with a good prognosis for return to athletic function in 3 horses with low-grade lameness and mild neurologic deficits. Arthroscopic removal of APJ fragments may be considered as an approach to treat these lesions, but a clear link between clinical signs and the fragments has not yet been proven. Surgical treatment of a larger number of horses will help to further establish the clinical significance of these osteochondral fragments in the cervical articular process joints.

7 Literaturverzeichnis

Ahmed M, Tameem E. (2017): Risk factors for adjacent segment disease development after cervical fusion. *J Orthop Skeletal Med* 1, 1-6

Aldrich E, Nout-Lomas Y, Seim HB III, Easley JT. (2018): Cervical stabilization with polyaxial pedicle screw and rod construct in horses: a proof of concept study. *Vet Surg* 47 (07), 932-941

Alta TD, Bell SN, Troupis JM, Coghlan JA, Miller D. (2012): The new 4-dimensional computed tomographic scanner allows dynamic visualization and measurement of normal acromioclavicular joint motion in an unloaded and loaded condition. *J Comput Assist Tomogr* 36, 749-754

Auer JA, Stick JA. (2018): *Equine Surgery*.
5., überarbeitete und aktualisierte Auflage, PA: Saunders; ISBN 978-0-323-48420-6

Beck C, Middleton D, Maclean A, Lavelle R. (2002): Osteochondrosis of the second cervical vertebra of a horse. *Equine Vet J* 34, 210-212

Beeres M, Wichmann JL, Paul J, Balisike M, Elsabaie M, Vogl TJ, Nour-Eldin A. (2015): CT chest and gantry rotation time: does the rotation time influence image quality? *Acta Radiol* 56, 950-954

Bergmann W, de Mik-van Mourik M, Veraa S. (2020): Cervical articular process joint osteochondrosis in Warmblood foals. *Equine Vet J*. 52 (5), 664-669

Birmingham SSW, Reed SM, Mattoon JS, Saville W. (2010): Qualitative assessment of corticosteroid cervical articular facet injection in symptomatic horses. *Equine Veterinary Education* 22, 77-82

Butler JA, Colles CM, Dyson SJ, Kold SE, Poulos PW. (2008): *Clinical Radiology of the Horse*
3., überarbeitete und aktualisierte Auflage, John Wiley & Sons, ISBN 978-1-11-891228-7

Choi YS, Lee YH, Kim S, Cho HW, Song HT, Suh JS. (2013): Four-dimensional real-time cine images of wrist joint kinematics using dual source CT with minimal time increment scanning. *Yonsei Med J* 54, 1026-1032

Cillan-Garcia E, Taylor SE, Townsend N, Licka T. (2011): Partial ostectomy of the dens to correct atlantoaxial subluxation in a pony. *Vet Surg.* 40, 596-600

Claridge HAH, Piercy RJ, Parry A, Weller R. (2010): The 3D anatomy of the cervical articular process joints in the horse and their topographical relationship to the spinal cord. *Equine Vet J.* 42, 726-731

Clayton HM, Townsend HG. (1989a): Kinematics of the cervical spine of the adult horse. *Equine Vet J* 21(03),189-192

Dawson P, Lees WR. (2001): Multi-slice technology in computed tomography. *Clin Radiol* 56,302-309

De Preux M, Klopfenstein Bregger MD, Brünisholz HP, Van der Vekens E; Schweizer-Gorgas D, Koch C. (2020): Clinical use of computer- assisted orthopedic surgery in horses. *Veterinary Surgery* 49, 1075-1087

De Lahunta A, Glass EN, Kent M. (2014b):
Veterinary Neuroanatomy and Clinical Neurology Elsevier, St. Louis,
4., überarbeitete und aktualisierte Auflage, Saunders (W.B.) Co Ltd (Verlag), ISBN 978-1-4557-4856-3

DeRouen A, Spriet M, Aleman M. (2016): Prevalence of anatomical variation of the sixth cervical vertebra and association with vertebral canal stenosis and articular process osteoarthritis in the horses. *Vet Radiol Ultrasound* 57, 253-258

Dimock AN, Puchalski SM. (2010): Clinical commentary: cervical radiology. *Equine Vet Educ.* 22,83-87

Dyson SJ.(2011): Lesions of the equine neck resulting in lameness or poor performance. *Vet Clin North Am Equine Pract.* 27 (3), 417-437

Dyson SJ. (2020): Unexplained forelimb lameness possibly associated with radiculopathy. *Equine Veterinary Education* 32, S10, 92-103

Dyson SJ. (2003): *Diagnosis and Management of Lameness in the Horse*. 2., überarbeitete und aktualisierte Auflage, St Louis, MO: Elsevier Science, ISBN 9781416060697

Edirisinghe Y, Troupis JM, Patel M, Smith J, Crossett M. (2014): Dynamic motion analysis of dart throwers motion visualized through computerized tomography and calculation of the axis of rotation. *J Hand Surg Eur Vol* 39, 364-372

Ehrle A, Jones SJ, Klose P, Lischer C. (2012): Atypical radiologic appearance of a second vertebral fracture in a horse. *J Equine Vet Sci.* 32, 309-313

Foss RR, Genetzky RM, Riedesel EA, Graham C. (1983): Cervical intervertebral disc protrusion in two horses. *Can Vet J* 24(06), 188-191

Fuentealba IC, Weeks BR, Martin MT, Joyce JR, Wease GS. (1991): Spinal cord ischemic necrosis due to fibrocartilaginous embolism in a horse. *J Vet Diagn Invest* 3(02), 176-179

Funk KA, Erickson ED. (1968): A case of atlantoaxial subluxation in a horse. *Can Vet J.* 9, 120-123

Furr MO, Anver M, Wise M. (1991): Intervertebral disk prolapse and diskospondylitis in a horse. *J Am Vet Med Assoc* 198(12), 2095-2096

Fürst A. AO Surgery Reference. Horse spine. <https://www2.aofoundation.org/wps/portal/surgery?showPage=approach&bone=HorseSpine&segment=Nonsegmented&Language=en>. Accessed June 28, 2019.

García-López JM. (2018): Neck, Back, and Pelvic Pain in Sport Horses. *Vet Clin North Am Equine Pract* 34, 235-251

Gasiorowski JC, Richardson DW. (2015): Clinical Use of Computed Tomography and Surface Markers to Assist Internal Fixation Within the Equine Hoof. *Veterinary Surgery* 44, 214-222

Gellman KS, Bertram JE. (2002): The equine nuchal ligament. 2. Passive dynamic energy exchange in locomotion. *Vet Comp Orthopaed* 15, 7-14

Gerlach K, Muggli L, Lempe A, Breuer J, Brehm W. (2012): Successful closed reduction of an atlantoaxial luxation in a mature warmblood horse. *Equine Vet Educ.* 24, 294-296

Grant BD, Barbee DD, Wagner PC (1985): Long term results of surgery for equine cervical vertebral malformation. *Proc Am Assoc Equine Pract* 31, 91-96

Grant GB, Bagby G, Rantanen N. (2003): Clinical results of kerf cylinder (Seattle Slew Implant) to reduce implant migration and fracture in horses undergoing surgical interbody fusion. *Vet Surg* 32, 499

Gondim Teixeira PA, Formery AS, Hossu G (2017): Evidence-based recommendations for musculoskeletal kinematic 4D-CT studies using wide area-detector scanners: a phantom study with cadaveric correlation. *Eur Radiol* 27, 437-446

Gough SL, Anderson JDC, Dixon JJ. (2020): Computed tomographic cervical myelography in horses: technique and findings in 51 clinical cases. *J Vet Intern Med.* 33, 377-386. <https://doi.org/10.1111/jvim.15848>

Grosjean R, Sauer B, Guerra RM. (2007): Degradation of the z- resolution due to a longitudinal motion with a 64-channel CT scanner. *Annu Int Conf IEEE Eng Med Biol Soc* 4429-4432

Guffy MM, Coffman JR, Strafuss AC. (1969): Atlantoaxial luxation in a foal. *J Am Vet Med Assoc.* 155, 754-757

Hakozaki T, Ichinohe T, Kanno N, Yogo T, Harada Y, Inaba T, Kasai Y, Hara Y. (2016): Biomechanical assessment of the effects of vertebral distraction-fusion techniques on the adjacent segment of canine cervical vertebrae. *Am J Vet Res* 77(11), 1194-1199

Henson FMD. (2018).

Equine Neck and Back Pathology.

2., überarbeitete und aktualisierte Auflage, Oxford: John Wiley & Sons Ltd, ISBN 978-1-118-97444-5

- Jackson MA, Ohlerth S, Fürst AE. (2019): Use of an aiming device and computed tomography for assisted debridement of subchondral cystic lesions in the limbs of horses. *Vet Surg* 48, 15-24
- Janes JG, Garrett KS, McQuerry KJ, Waddell S, Voor MJ, Reed SM, Williams NM, McLeod JN. (2015): Cervical vertebral lesions in equine stenotic myelopathy. *Vet Pathol.* 52 (5), 919-927
- Keller SA, Fürst AE, Kircher P, Ringer S, Kuemmerle JM. (2015): Locking compression plate fixation of equine tarsal subluxations. *Vet Surg.* 44, 949-957
- Kerkhof FD, Brugman E, D'Agostino P, Dourthe B, van Lenthe GH, Stockmans F, Jonkers I, Vereecke EE. (2016): Quantifying thumb opposition kinematics using dynamic computed tomography. *J Biomech* 49, 1994-1999
- Krüger W. (1939): Über Schwingungen der Wirbelsäule – Insbesondere der Wirbelbrücke des Pferdes während der Bewegung. *Berl Munch Tierarztl Wochenschr* 13, 129-133
- Kühnle C, Fürst A, Kümmerle J. (2018): Outcome of ventral fusion of two or three cervical vertebrae with a locking compression plate in 8 horses. *Vet Comp Orthop Traumatol.* 3, 356-363
- Kwong Y, Mel AO, Wheeler G, Troupis JM. (2015): Four-dimensional computed tomography (4DCT): A review of the current status and applications. *J Med Imaging Radiat Oncol* 59, 545-554
- Leng S, Zhao K, Qu M, An KN, Berger R, McCollough CH. (2011): Dynamic CT technique for assessment of wrist joint instabilities. *Med Phys* 38 Suppl 1, S50
- Levine JM, Levine GJ, Hoffman AG, Mez J, Bretton GR. (2007): Comparative anatomy of the horse, ox, and dog: the vertebral column and peripheral nerves. *Compend Equine* 1, 279-292
- Licka T, Edinger H. (2002): Temporary successful closed reduction of an atlantoaxial luxation in a horse. *Vet Comp Orthop Traumatol.* 13, 146-148
- Licka T. (2002): Closed reduction of an atlanto-occipital and atlantoaxial dislocation in a foal. *Vet Rec.* 151, 356-357

Lim CK, Hawkins JF, Vanderpool AL, Heng HG, Gillespie Harmon CC, Lenz SD. (2017): Osteochondritis dissecans-like lesions of the occipital condyle and cervical articular process joints in a Saddlebred colt horse. *Acta Vet Scand.* 59 (1), 76

Lindgren CM, Wright L, Kristoffersen M, Puchalski SM. (2020): Computed tomography and myelography of the equine cervical spine: 180 cases (2013–2018). *Equine Vet Educ.* 33(9) 475-483. doi: 10.1111/eve.13350

Lischer C, Rossignol F, Watkins JP. (2019): AOTK System Innovations. 2018.
<https://view.joomag.com/aotk-system-innovations-2018-aotk-innovations-2018/0399541001544026356>.

Matsunaga S, Kabayama S, Yamamoto T, Yone K, Sakou T, Nakanishi K. (1999): Strain on intervertebral discs after anterior cervical decompression and fusion. *Spine* 24(07), 670-675

Mattoon JS, Drost WT, Grguric MR, Auld DM, Reed SM. (2004): Technique for equine cervical articular process joint injection. *Vet. Radiol. Ultrasound* 40, 238-240

Mayhew IG, De Lahunta A, Whitlock RH. (1978): Spinal cord diseases in the horse. *Cornell Vet.* 68, Suppl. 6, 1-207

Mayhew IG, Donawick WJ, Green SL. (1993): Diagnosis and prediction of cervical vertebral malformation in thoroughbred foals based on semiquantitative radiographic indicators. *Equine Vet. J.* 25, 435-440

McCoy DJ, Shires PK, Beadle R. (1984): A ventral approach for stabilization of atlantoaxial subluxation secondary to an odontoid fracture in a foal. *J Am Vet Med Assoc.* 185, 545-549

McIlwraith, CW and Trotter, GW. (1996):

Joint Disease in the Horse.

2., überarbeitete und aktualisierte Auflage, W.B. Saunders, Philadelphia, ISBN 9781455759699

McIlwraith CW, Foerner JJ, Davis DM. (1991): Osteochondritis dissecans of the tarsocrural joint: results of treatment with arthroscopic surgery. *Equine Vet J.* 23, 155-162

McIlwraith CW. (2013): Surgical versus conservative management of osteochondrosis. *Vet J.* 197, 19-28

McIlwraith CW, Billingham RC, Frisbie DD. (2001): Current and future diagnostic means to better characterise osteoarthritis in the horse - Routine synovial fluid analysis and synovial fluid and serum markers. *Proc. Am. Ass. equine Practnrs.* 47, 171-179

Mosby (2013):

Mosby's Medical Dictionary.

9., überarbeitete und aktualisierte Auflage, St. Louis: Mosby Elsevier

Moore BR, Reed SM, Robertson JT. (1993): Surgical treatment of cervical stenotic myelopathy in horses: 73 cases (1983-1992). *J Am Vet Med Assoc* 203 (01), 08-112

Moore BR, Holbrook TC, Stefanacci JD, Reed SM, Tate LP, Menard MC. (1992): Contrast-enhanced computed tomography and myelography in six horses with cervical stenotic myelopathy. *Equine vet. J.* 24, 197-202

Moore BR, Reed SM, Biller DS, Kohn CW, Weisbrode SE. (1994): Assessment of vertebral canal diameter and bony malformations of the cervical part of the spine in horses with cervical stenotic myelopathy. *Am. J. vet. Res.* 55, 5-13

Nickel R, Schummer A, Seiferle E. (1986):

Lehrbuch der Anatomie der Haustiere.

8., überarbeitete und aktualisierte Auflage, Berlin: Verlag Paul Parley, ISBN 9783830441502

Nixon AJ, Stashak TS. (1985): Surgical therapy for spinal cord disease in the horse. *Proc Am Assoc Equine Pract* 31, 61-74

Nixon AJ, Stashak TS, Ingram J. (1982): Diagnosis of cervical vertebral malformation in the horse. *Proc. Am. Ass. equine Practnrs.* 28, 253-266

Nixon AJ. (1996):

Equine Fracture Repair.

2., überarbeitete und aktualisierte Auflage, Philadelphia, PA: WB Saunders, ISBN 978-0-7216-6754-6

Nixon AJ, Stashak TS. (1988): Laminectomy for relief of atlantoaxial subluxation in four horses. *J Am Vet Med Assoc.* 193, 677-682

Nixon AJ. (1991): Surgical management of equine cervical vertebral malformation. *Prog Vet Neurol.* 2, 183-195

Nout YS and Reed SM. (2002): Cervical vertebral stenotic myelopathy. *Equine Vet. Educ.* 15, 212-223

O'Leary SA, White JL, Hu JC, Athanasiou KA. (2018): Biochemical and biomechanical characterization of equine cervical facet joint cartilage. *Equine Vet J.* 50, 800-808

Pepe M, Angelone M, Gialletti R, Nannarone S, Beccati F. (2014): Arthroscopic anatomy of the equine cervical articular process joints. *Equine Vet J.* 46, 345-351

Pérez-Nogués M, Vaughan B, Phillips KL, Galuppo LD. (2020): Evaluation of the caudal cervical articular process joints by using a needle arthroscope in standing horses. *Veterinary Surgery* 49, 463-471

Pool RR. (1993): Difficulties in definition of equine osteochondrosis; differentiation of developmental and acquired lesions. *Equine Vet J Suppl.* 16, 5-12

Powers BE, Stashak TS, Nixon AJ, Yovich JV, Nordin RW. (1988): Pathology of the vertebral column of horses with cervical static stenosis. *Vet Pathol.* 23, 392-399

Puchalski SM, Galuppo LD, Hornof WJ, Wisner ER. (2007): Intraarterial contrast-enhanced computed tomography of the equine distal extremity. *Vet Radiol Ultrasound* 48, 21-29

Reardon R, Kummer M, Lischer C. (2009): Ventral locking compression plate for treatment of cervical stenotic myelopathy in a 3-month- old warmblood foal. *Vet Surg* 38 (04), 537-542

Reardon RJ, Bailey R, Walmsley JP, Heller J, Lischer C.(2010): An in vitro biomechanical comparison of a locking compression plate fixation and kerf cut cylinder fixation for ventral arthrodesis of the fourth and the fifth equine cervical vertebrae. *Vet Surg* 39 (08), 980-990

Ricardi G, Dyson SJ. (1993): Forelimb lameness associated with radiographic abnormalities of the cervical vertebrae. *Equine Vet J.* 25 (5), 422-426

Ricardi G, Dyson SJ. (1993): Forelimb lameness associated with radiographic abnormalities of the cervical vertebrae. *Equine Vet J* 25, 422-426

Rooney JR. (1975): Osteochondrosis in the horse. *Mod Vet Pract.* 56,41-43

Rüedi M, Hagen R, Lüchinger U, Fürst A, Trump M. (2011): Subluxation von C2 und C3 und Fraktur von C2 nach einem schweren Schädelhirntrauma bei zwei Warmblutpferden. *Pferdeheilkunde* 27, 522-527

Schulze N, Ehrle A, Weller R, Fritsch G, Gernhardt J, Ben Romdhane R, Lischer C. (2020): Computed Tomographic Evaluation of Adjacent Segment Motion after Ex Vivo Fusion of Equine Third and Fourth Cervical Vertebrae. *Vet Comp Orthop Traumatol* 33, 1-8

Schütte A. (2005): Untersuchungen zum equinen wobbler syndrom. (Examination of the equine wobbler syndrome). Doctoral thesis, Munich, Germany: Ludwig-Maximilians-Universität

Schwab JS, Diangelo DJ, Foley KT. (2006): Motion compensation associated with single-level cervical fusion: where does the lost motion go? *Spine* 31(21), 2439-2448

Sleutjens J, Cooley AJ, Sampson SN, Wijnberg ID, Back W, van der Kolk JH, Swiderski CE. (2014): The equine cervical spine: comparing MRI and contrast-enhanced CT images with anatomic slices in the sagittal, dorsal, and transverse plane. *Vet Q* 34, 74-84

Slone DE, Bergfeld WA, Walker TL. (1973): Surgical decompression for traumatic atlantoaxial subluxation in a weanling filly. *J Am Vet Med Assoc.*174, 1234-1236

Stewart RH, Reed SM, Weisbrode SE. (1991): Frequency and severity of osteochondrosis in horses with cervical stenotic myelopathy. *Am J Vet Res* 52, 873-879

Szklarz M, Skalec A, Kirstein K. (2018): Management of equine ataxia caused by cervical vertebral stenotic myelopathy: a European perspective 2010-2015. *Equine Vet Educ* 30, 370-376

Tay SC, Primak AN, Fletcher JG, Schmidt B, Amrami KK, Berger RA, McCollough CH. (2007): Four-dimensional computed tomographic imaging in the wrist: proof of feasibility in a cadaveric model. *Skeletal Radiol* 36, 1163-1169

Thomsen LN, Berg LC, Markussen B, Thomsen PD. (2013): Synovial folds in equine articular process joints. *Equine Veterinary Journal* 45, 448-453

Totterman S, Tamez-Pena J, Kwok E, Strang J, Smith J, Rubens D, Parker K. (1998): 3D visual presentation of shoulder joint motion. *Stud Health Technol Inform* 50, 27-33

Trostle S, Dubielzig R, Beck K. (1993): Examination of frozen cross sections of cervical spinal intersegments in nine horses with cervical vertebral malformation: lesions associated with spinal cord compression. *J Vet Diagn Invest.* 5, 423-431

Tucker R, Piercy RJ, Dixon JJ, Muir CF, Smith KC, Potter KE, Leaman TR, Smith RKW. (2018): Arthroscopic treatment of cervical articular process joint osteochondrosis in a thoroughbred horse. *Equine Vet Educ.* 30, 116-121

Tucker R, Hall YS, Hughes TK, Parker RA. (2021): Osteochondral fragmentation of the cervical articular process joints. *Equine Vet J.* 54, 106-113. DOI: 10.1111/evj.13410

Van Biervliet J, Mayhew J, De Lahunta A. (2006): Cervical vertebral compressive myelopathy: diagnosis. *Clin. Tech. Equine Pract.* 5, 54-59

Volkheimer D, Malakoutian M, Oxland TR, Wilke HJ. (2015): Limitations of current in vitro test protocols for investigation of instrumented adjacent segment biomechanics: critical analysis of the literature. *Eur Spine J* 24(09), 1882-1892

Vaughan LC, Mason BJE. (1973): *A Clinico-Pathological Study of Racing Accidents in Horses: A Report of a Study on Equine Fatal Accidents on Racecourses Financed by the Horserace Betting Levy Board.* Vol 1973. Dorking, United Kingdom: Bartholomew Press:1-88.

Walmsley JP. (2005): Surgical treatment of cervical spinal cord compression in horses: a European experience. *Equine Vet Educ* 17, 39-43

Wassilew GI, Janz V, Heller MO, Tohtz S, Rogalla P, Hein P, Perka C. (2013): Real time visualization of femoroacetabular impingement and subluxation using 320-slice computed tomography. *J Orthop Res* 31, 275-281

White J, Couzens G, Jeffery C. (2019): The use of 4D-CT in assessing wrist kinematics and pathology: a narrative view. *Bone Joint J* 101-b, 1325-1330

Whithers JM, Voute LC, Hammond G, Lischer CJ. (2009): Radiographic anatomy of the articular process joints of the caudal cervical vertebrae in the horse on lateral and oblique projections. *Equine Vet J.* 41, 895-902

Wissdorf H, Gerhards H, Huskamp B, Deegen E. (2010):
Praxisorientierte Anatomie und Propädeutik des Pferdes.
3, überarbeitete und aktualisierte Auflage, Hannover: Schaper M. & H, ISBN 3794402162

Witte S, Alexander K, Bucellato M. (2005): Congenital atlantoaxial luxation associated with malformation of the dens axis in a quarter horse foal. *Equine Vet Educ.* 17, 175-178

Yoon DH, Yi S, Shin HC, Kim KN, Kim SH. (2006): Clinical and radiological results following cervical arthroplasty. *Acta Neurochir (Wien)* 148 (09), 943-950

Zsoldos RR, Licka TF. (2015): The equine neck and its function during movement and locomotion. *Zoology (Jena)* 118 (05), 364-376

Zsoldos RR, Groesel M, Kotschwar A, Kotschwar AB, Licka T, Peham C. (2010): A preliminary modelling study on the equine cervical spine with inverse kinematics at walk. *Equine Vet J Suppl* 42 (38), 516-522

8 List of publications and oral presentations

- Schulze N, Werpy N, Gernhardt J, Fritsch G, Hildebrandt T, Vanderperren K, Klopffleisch R, Ben Romdhane R, Lischer C, Ehrle A. Dynamic three-dimensional computed tomographic imaging facilitates evaluation of the equine cervical articular process joint in motion. *Equine Veterinary Journal*. 2022.
- Schulze N, Ehrle A, Beckmann I, Lischer C. Arthroscopic removal of osteochondral fragments of the cervical articular process joints in three horses. *Veterinary Surgery*. 2021;1-9. <https://doi.org/10.1111/VSU.13681>
- Schulze N, Ehrle A, Weller R, Fritsch G, Gernhardt J, Ben Romdhane R, Lischer C. Computed Tomographic Evaluation of Adjacent Segment Motion after Ex Vivo Fusion of Equine Third and Fourth Cervical Vertebrae. *VCOT 2020* <https://doi.org/10.1055/s-0039-1693665>. ISSN 0932-0814.
- Schulze N, Ehrle A, Noguera Cordero AC, Lischer C. Internal fixation of a complete ventral luxation of the dens axis in an American quarter horse yearling. *Veterinary Surgery*. 2019;1–7. <https://doi.org/10.1111/vsu.13283>
- Oral presentation Resident Forum Annual Scientific Meeting ECVS Budapest 2019 "Computed Tomographic Evaluation of Adjacent Segment Motion after Ex Vivo Fusion of Equine Third and Fourth Cervical Vertebrae"
- Abstract: "Evaluation of range of motion of adjacent cervical vertebral segments after surgical fusion of C3/4 in the horse using 3D and 4D computed tomography" submitted for presentation at the ECVS Annual Scientific Meeting 2019, Budapest, Hungary
- Oral presentation Master Modul Equine Berlin "Orthopaedics" 2019 "Ligament and Tendon Diseases"
- Oral presentation Master Modul Equine Berlin "Orthopaedics" 2019 "Emergency Treatment and Transportation"
- Oral presentation Master Modul Equine Berlin "Gastroenterology" 2018 "Sinus disease – Case examples"

- Oral presentation Master Modul Equine Berlin “Gastroenterology” 2018
“Diagnosis of dental related sinus diseases”
- Winner “ECVS Resident Research Grant”, April 2017
- Schulze N, Lischer C. The scientific background for the classification of findings in the german guidelines for scoring prepurchase radiographs in the horse - Part II the proximal phalanx and the proximal sesamoid bones, Pferdeheilkunde 6/2016
- Schulze N, Lischer C. The scientific background for the classification of findings in the german guidelines for scoring prepurchase radiographs in the horse - Part I the fetlock joint, Pferdeheilkunde 3/2016

9 Danksagung

Zuallererst möchte ich Prof. Christoph Lischer, für die neun lehrreichen Jahre danken, die wir zusammen in der Klinik verbracht haben. Ich möchte Ihnen dafür danken, dass Sie mir die Möglichkeit gegeben haben dieses spannende Thema so intensiv zu bearbeiten und ich danke Ihnen für all die Geduld, die Sie mit mir hatten.

Ein großer Dank geht auch an meine beiden Betreuer Prof. Renate Weller und Prof. Robert Klopfeisch. Vielen Dank für die Hilfe und Unterstützung bei der Erstellung dieser Arbeit.

Ebenfalls bedanken möchte ich mich bei Prof. Natasha Werpy für die Unterstützung bei der Auswertung der Bilder und den Glauben an dieses Projekt.

Auch bei dem Leibniz-Institut für Zoo- und Wildtierforschung in Berlin und Prof. Katrien Vanderperren möchte ich mich herzlich für die Unterstützung bedanken.

Des Weiteren gilt mein Dank Jennifer Gernhardt. Vielen Dank Jenny, für die vielen tollen gemeinsamen Stunden im Keller, deine leckeren Kuchen und deine unermüdliche Hilfe. Ein großer Dank geht auch an Alexander Gernhardt ohne dessen innovative Umsetzung dieses Projekt nicht möglich gewesen wäre.

Bedanken möchte ich mich auch bei Anna Ehrle, für ihre tatkräftige Unterstützung.

Last but not least möchte ich noch meinem Thorben danken. Jeder Skeptiker braucht einen Visionär.

10 Funding Sources

Funding for this study was provided by the European College of Veterinary Surgeons (ECVS Residents Research Grant).

11 Conflict of Interest

No conflict of interest.

12 Selbstständigkeitserklärung

Hiermit bestätige ich, dass ich die vorliegende Arbeit selbstständig angefertigt habe. Ich versichere, dass ich ausschließlich die angegebenen Quellen und Hilfen in Anspruch genommen habe.

Berlin, den 12. Oktober 2022

Nicole Schulze

